JOURNAL OF PETROLOGY | VOLUME 45 | NUMBER 9 | PAGES 1907–1921 | 2004 | DOI: 10.1093/petrology/egh038

Empirical Garnet–Biotite–Plagioclase–Quartz (GBPQ) Geobarometry in Medium- to High-Grade Metapelites*

CHUN-MING WU[1]†, JIAN ZHANG[1] AND LIU-DONG REN[2]

[1]LABORATORY OF COMPUTATIONAL GEODYNAMICS, THE GRADUATE SCHOOL, CHINESE ACADEMY OF SCIENCES, PO BOX 3908, BEIJING 100039, CHINA

[2]INSTITUTE OF GEOLOGY, CHINESE ACADEMY OF GEOLOGICAL SCIENCES, 26 BAIWANZHUANG STREET, BEIJING 100037, CHINA

RECEIVED AUGUST 7, 2003; ACCEPTED APRIL 6, 2004
ADVANCE ACCESS PUBLICATION JULY 29, 2004

On the basis of the net transfer reactions among garnet, biotite, plagioclase and quartz (for both Mg and Fe end-member models), the garnet–biotite–plagioclase–quartz (GBPQ) geobarometer was empirically calibrated under physical conditions of P = *1·0–11·4 kbar and* T = *515–878°C, based on the input garnet–biotite temperatures and garnet–aluminosilicate–plagioclase–quartz (GASP) pressures of 224 natural aluminosilicate-bearing metapelitic samples collated from the literature. The calibrations are internally consistent with the asymmetric quaternary solid solution model of garnet, the symmetric quaternary solid solution model of biotite, and the Al-avoidance ternary solid solution model of plagioclase in calibrating the garnet–biotite geothermometer and the GASP geobarometer. The resulting two GBPQ barometer formulae reproduce the input GASP pressures well within ±1·0 kbar (mostly within ±0·5 kbar). For both aluminosilicate-bearing and aluminosilicate-absent metapelites, the two GBPQ barometry formulae yielded identical pressures, whether the sample was included or not included in calibrating the GBPQ barometry. The random error of the GBPQ barometry may be expected as ±1·2 kbar. The* d*P*/d*T slopes of these two GBPQ formulae are close to that of the GASP barometer in* P–T *space. Applications of the GBPQ barometry of aluminosilicate-absent metapelites to the rocks within a thermal contact aureole, or rocks within a limited geographical area without post-metamorphic structural discontinuity, show no obvious pressure change. It may be concluded that the two GBPQ barometry formulae derived in this study may be used as practical tools for metamorphic pelites under the conditions of 515–878°C and 1·0–11·4 kbar, in the composition range of* $X_{gros} > 3\%$ *in garnet,* $X_{an} > 17\%$ *in plagioclase, and* $X_{Al}^{bio} > 3\%$ *in biotite. Application of the GBPQ barometer beyond the calibration range should be undertaken with caution.*

KEY WORDS: *applicability; calibration; geobarometry; metapelite*

(A11). INTRODUCTION

Aluminosilicate minerals, which have been studied extensively, are not always present in metapelites. In this case the widely used garnet–aluminosilicate–plagioclase–quartz (GASP) barometer cannot be applied, and aluminosilicate-free geobarometers are necessary. In this paper, we calibrated the garnet–biotite–plagioclase–quartz (GBPQ) barometer, so that it may be applied to metapelites, especially when aluminosilicate is absent.

Geobarometers for the pelitic mineral assemblage garnet + biotite + plagioclase + muscovite + quartz have been calibrated by several workers (e.g. Ghent & Stout, 1981; Hodges & Crowley, 1985; Holdaway *et al.*, 1988; Hoisch, 1990, 1991; McMullin *et al.*, 1991). At present, the recently calibrated garnet–biotite thermometer (Holdaway, 2000) and the GASP barometer (Holdaway, 2001) yield *P–T* estimates for both experimental charges and natural rock assemblages that are much more precise than those obtained using alternative calibrations, therefore they are the best basis for the calibration of the GBPQ barometry.

There are nearly 30 versions of the garnet–biotite thermometer at present, among which the Holdaway (2000) version yields the smallest absolute error (±25°C) in

*In honour of Professor Yusheng Pan.

†Corresponding author. Telephone: 86-10-88256312. Fax: 86-10-88256012. E-mail: wucm@gscas.ac.cn

reproducing the experimental temperatures of Ferry & Spear (1978) and Perchuk & Lavrent'eva (1983), in the wide temperature range 550–950°C. Furthermore, this thermometer may successfully discern the systematic change of temperatures in metapelites from different zones of prograde sequences (e.g. Ferry, 1980; Lang & Rice, 1985; Gordon *et al.*, 1991; Boyle & Westhead, 1992; Huang *et al.*, 2003), inverted metamorphic zones (e.g. Himmelberg *et al.*, 1991; Swapp & Hollister, 1991; Spear *et al.*, 1995; Stephenson *et al.*, 2000), and thermal contact aureoles (e.g. Delor *et al.*, 1984; Barboza & Bergantz, 2000; Mezger *et al.*, 2001). Therefore this thermometer is believed to be a reliable and precise tool. Meanwhile, the new GASP barometer (Holdaway, 2001) has a small absolute error of ±0·8 kbar in reproducing the experimental pressures (Hays, 1966; Hariya & Kennedy, 1968; Goldsmith, 1980; Gasparik, 1984; Koziol & Newton, 1988), and can precisely determine the reliable sillimanite–kyanite transition boundary for 76 metapelitic samples from 11 localities (Holdaway, 2001, and reference therein) and Alpine metapelites (Engi *et al.*, 1995; Todd & Engi, 1997), and thus is believed to be a reliable barometer.

Geobarometers involving mineral assemblages that are more common, but not easily calibrated experimentally, may sometimes be calibrated empirically (Hoisch, 1990). Because at present there are no experiments to calibrate the GBPQ barometer, in this study we empirically calibrated it on the basis of the garnet–biotite thermometer and the GASP barometer. First, we collected data for 224 aluminosilicate-bearing metapelites from the literature to calibrate the GBPQ barometer. Second, we used an additional 89 aluminosilicate-bearing metapelites not included in the calibration, to test the validity of the GBPQ barometer. Third, we applied the GBPQ barometer to aluminosilicate-bearing and/or aluminosilicate-absent metapelites within thermal contact aureoles, and those within a limited geographical area without post-metamorphic structural discontinuity, to test the applicability of the GBPQ barometer. The results show that the GBPQ barometer derived in this study may be accurately applied to either aluminosilicate-bearing or aluminosilicate-free, medium- to high-grade metapelites.

THERMODYNAMIC BACKGROUND

Thermodynamic models

The GBPQ barometry is based on the following Mg- and Fe-model equilibria (e.g. Hoisch, 1990, 1991):

$$\underset{\text{pyrope}}{Mg_3Al_2Si_3O_{12}} + 2\underset{\text{grossular}}{Ca_3Al_2Si_3O_{12}} + 3K\underset{\text{eastonite}}{(Mg_2Al)(Si_2Al_2)O_{10}(OH)_2} + 6\underset{\text{quartz}}{SiO_2} = 6\underset{\text{anorthite}}{CaAl_2Si_2O_8} + 3K\underset{\text{phlogopite}}{Mg_3(AlSi_3)O_{10}(OH)_2} \quad (1)$$

and

$$\underset{\text{almandine}}{Fe_3Al_2Si_3O_{12}} + 2\underset{\text{grossular}}{Ca_3Al_2Si_3O_{12}} + 3K\underset{\text{siderophyllite}}{(Fe_2Al)(Si_2Al_2)O_{10}(OH)_2} + 6\underset{\text{quartz}}{SiO_2} = 6\underset{\text{anorthite}}{CaAl_2Si_2O_8} + 3K\underset{\text{annite}}{Fe_3(AlSi_3)O_{10}(OH)_2}. \quad (2)$$

At equilibrium, when ignoring heat capacity, thermal expansion and compressibility of the phases involved, and assuming quartz to be a pure phase, the above two model reactions may be described respectively by the following two thermodynamic equations:

$$\Delta_1 G = 0 = \Delta_1 H^0 - T\cdot\Delta_1 S^0 + (P-1)\cdot\Delta_1 V^0 + RT\ln K^{\text{ideal}}_{(1)} + 6RT\ln\gamma^{\text{pl}}_{\text{an}} + 3RT\ln(\gamma^{\text{bio}}_{\text{phl}}/\gamma^{\text{bio}}_{\text{eas}}) - 2RT\ln\gamma^{\text{grt}}_{\text{gros}} - RT\ln\gamma^{\text{grt}}_{\text{pyr}} \quad (3)$$

and

$$\Delta_2 G = 0 = \Delta_2 H^0 - T\cdot\Delta_2 S^0 + (P-1)\cdot\Delta_2 V^0 + RT\ln K^{\text{ideal}}_{(2)} + 6RT\ln\gamma^{\text{pl}}_{\text{an}} + 3RT\ln(\gamma^{\text{bio}}_{\text{ann}}/\gamma^{\text{bio}}_{\text{sid}}) - 2RT\ln\gamma^{\text{grt}}_{\text{gros}} - RT\ln\gamma^{\text{grt}}_{\text{alm}}. \quad (4)$$

In the above two equations the subscripts 1 and 2 refer to reaction (1) and reaction (2), respectively. ΔG is Gibbs free energy of the respective reaction at the P and T of interest. $K^{\text{ideal}}_{(1)}$ and $K^{\text{ideal}}_{(2)}$ are the respective equilibrium constants expressed as the products of ideal activities of the phases involved in each of the above two reactions, and these terms and the ideal activity models of the phases involved are defined in Table 1. The γ terms refer to the activity coefficients of the mineral components. In the equilibria expressions, ΔH^0, ΔS^0 and ΔV^0 refer to net changes in enthalpy, entropy and volume of the reactions involving pure phases at the standard state (298·15 K and 1 bar), respectively. It has been assumed that heat capacity, thermal expansion and compressibility of the reactions may be neglected, and this implies that ΔH^0, ΔS^0 and ΔV^0 do not vary or that any variation cancels out in the calibration range of pressure and temperature. For reactions involving only solid phases, this is a common and reasonable practice, which leads to negligible errors in P–T estimation.

Activity model of garnet

Holdaway (2000, 2001) used the garnet activity models of Berman & Aranovich (1996), Ganguly *et al.* (1996) and Mukhopadhyay *et al.* (1997), and an average model of the three. After comparing the garnet–biotite temperatures and the temperatures of garnet–biotite Fe–Mg exchange experiments (Ferry & Spear, 1978; Perchuk & Lavrent'eva, 1983), the average garnet model was preferred (Holdaway, 2000).

Table 1: Ideal activity of the mineral phases and equilibrium constants of the model reactions

Garnet

$X^{grt}_{alm} = (X^{grt}_{Fe})^3$, $X^{grt}_{pyr} = (X^{grt}_{Mg})^3$, $X^{grt}_{gros} = (X^{grt}_{Ca})^3$, $X^{grt}_{sps} = (X^{grt}_{Mn})^3$

$X^{grt}_{Fe} = Fe^{2+}/(Fe^{2+} + Mg + Ca + Mn)$, $X^{grt}_{Mg} = Mg/(Fe^{2+} + Mg + Ca + Mn)$

$X^{grt}_{Ca} = Ca/(Fe^{2+} + Mg + Ca + Mn)$, $X^{grt}_{Mn} = Mn/(Fe^{2+} + Mg + Ca + Mn)$

Biotite

$X^{bio}_{ann} = (X^{bio}_{Fe})^3$, $X^{bio}_{phl} = (X^{bio}_{Mg})^3$, $X^{bio}_{eas} = \frac{27}{4}(X^{bio}_{Mg})^2 X^{bio}_{Al}$

$X^{bio}_{sid} = \frac{27}{4}(X^{bio}_{Fe})^2 X^{bio}_{Al}$

$X^{bio}_{Fe} = Fe^{2+}/(Fe^{2+} + Mg + Al^{VI} + Ti)$, $X^{bio}_{Mg} = Mg/(Fe^{2+} + Mg + Al^{VI} + Ti)$

$X^{bio}_{Al} = Al^{VI}/(Fe^{2+} + Mg + Al^{VI} + Ti)$, $X^{bio}_{Ti} = Ti/(Fe^{2+} + Mg + Al^{VI} + Ti)$

Plagioclase

$X^{pl}_{an} = 0{\cdot}25X^{pl}_{Ca}(1 + X_{Ca})^2$, $X^{pl}_{ab} = X^{pl}_{Na}$, $X^{pl}_{or} = X^{pl}_{K}$

$X^{pl}_{Ca} = Ca/(Ca + Na + K)$, $X^{pl}_{Na} = Na/(Ca + Na + K)$

$X^{pl}_{K} = K/(Ca + Na + K)$

Equilibrium constants

$$K^{ideal}_{(1)} = \frac{(X^{pl}_{an})^6(X^{bio}_{phl})^3}{(X^{grt}_{pyr})(X^{grt}_{gros})^2(X^{bio}_{eas})^3(X^{qtz}_{qtz})^6} = \frac{(X^{pl}_{Ca})^6(1 + X^{pl}_{Ca})^{12}(X^{bio}_{Mg})^3}{1259712{\cdot}0(X^{grt}_{Mg})^3(X^{grt}_{Ca})^6(X^{bio}_{Al})^3}$$

$$K^{ideal}_{(2)} = \frac{(X^{pl}_{an})^6(X^{bio}_{ann})^3}{(X^{grt}_{alm})(X^{grt}_{gros})^2(X^{bio}_{sid})^3(X^{qtz}_{qtz})^6} = \frac{(X^{pl}_{Ca})^6(1 + X^{pl}_{Ca})^{12}(X^{bio}_{Fe})^3}{1259712{\cdot}0(X^{grt}_{Fe})^3(X^{grt}_{Ca})^6(X^{bio}_{Al})^3}$$

Subsequently, after inspecting the locations of the kyanite–sillimanite boundary determined by several GASP formulae for the 76 samples from 11 localities (Holdaway, 2001, and reference therein), again, the average model was preferred (Holdaway, 2001). Following Holdaway (2000, 2001), we used the average garnet activity model in the calibration of the GBPQ barometry. For the construction of formulation of both the Fe–Mg–Ca–Mn quaternary garnet solid solution and the Fe–Mg–Al–Ti quaternary biotite solid solution, the activity coefficient formulation for quaternary solid solution of Mukhopadhyay *et al.* (1993) was adopted, in accordance with Holdaway (2000, 2001). The activity coefficients of the grossular, pyrope and almandine end-members in garnet, after rearrangement, may be written respectively as

$$RT\ln\gamma^{grt}_{gros} = 3RT\ln(\gamma^{grt}_{Ca}) = Caa \cdot T(K) + Cab \cdot P(bars) + Cac \quad (5)$$

$$RT\ln\gamma^{grt}_{pyr} = 3RT\ln(\gamma^{grt}_{Mg}) = Mga \cdot T(K) + Mgb \cdot P(bars) + Mgc \quad (6)$$

$$RT\ln\gamma^{grt}_{alm} = 3RT\ln(\gamma^{grt}_{Fe}) = Fea \cdot T(K) + Feb \cdot P(bars) + Fec \quad (7)$$

in which Caa, Cab, Cac, Fea, Feb, Fec, Mga, Mgb and Mgc are polynomial expressions for the end-members of garnet and are described in the Appendix.

Activity model of plagioclase

Following Holdaway (2001), we used the Al-avoidance activity model of plagioclase (Fuhrman & Lindsley, 1988). Rearranging the expression in Fuhrman & Lindsley's (1988) model, the activity coefficient of anorthite in plagioclase is expressed as

$$RT\ln(a^{pl}_{An}) = RT\ln[0{\cdot}25X^{pl}_{Ca}(1 + X^{pl}_{Ca})^2] + T(K) \cdot Fa + P(bars) \cdot Fb + Fc \quad (8)$$

in which Fa, Fb and Fc are polynomial expressions for the end-members of plagioclase and are described in the Appendix.

Activity model of biotite

Holdaway (2000) derived the following Margules parameters for non-ideal mixing in biotite in calibrating the garnet–biotite thermometer:

$$W^{bio}_{FeMg} = 22998{\cdot}0 - 17{\cdot}396T(K)\ \ J/mol \quad (9)$$

$$W^{bio}_{FeAl} - W^{bio}_{MgAl} = 245559{\cdot}0 - 280{\cdot}306T(K)\ \ J/mol \quad (10)$$

$$W^{bio}_{FeTi} - W^{bio}_{MgTi} = 310990{\cdot}0 - 370{\cdot}39T(K)\ \ J/mol. \quad (11)$$

According to the symmetric quaternary solid solution theory of Mukhopadyay *et al.* (1993), and inserting the above Margules parameters [equations (9)–(11)] of biotite (Holdaway, 2000), the ratio of activity coefficients of phlogopite and eastonite and annite and siderophyllite in biotite may be described respectively as

$$\begin{aligned} RT\ln(\gamma^{bio}_{phl}/\gamma^{bio}_{eas}) &= W^{bio}_{MgAl}(X^{bio}_{Al} - X^{bio}_{Mg}) + (W^{bio}_{FeMg} - W^{bio}_{FeAl})X^{bio}_{Fe} \\ &\quad + (W^{bio}_{MgTi} - W^{bio}_{AlTi})X^{bio}_{Ti} \\ &= W^{bio}_{MgAl}(X^{bio}_{Al} - X^{bio}_{Fe} - X^{bio}_{Mg}) + (W^{bio}_{MgTi} - W^{bio}_{AlTi})X^{bio}_{Ti} \\ &\quad + [-222561{\cdot}0 + 262{\cdot}91T(K)]X^{bio}_{Fe} \end{aligned} \quad (12)$$

and

$$\begin{aligned} RT\ln(\gamma^{bio}_{ann}/\gamma^{bio}_{sid}) &= W^{bio}_{FeAl}(X^{bio}_{Al} - X^{bio}_{Fe}) + (W^{bio}_{FeMg} - W^{bio}_{AlMg})X^{bio}_{Mg} \\ &\quad + (W^{bio}_{FeTi} - W^{bio}_{AlTi})X^{bio}_{Ti} \\ &= W^{bio}_{MgAl}(X^{bio}_{Al} - X^{bio}_{Fe} - X^{bio}_{Mg}) + (W^{bio}_{MgTi} - W^{bio}_{AlTi})X^{bio}_{Ti} \\ &\quad - 245559{\cdot}0X^{bio}_{Fe} + 22998{\cdot}0X^{bio}_{Mg} + 245559{\cdot}0X^{bio}_{Al} \\ &\quad + 310990{\cdot}0X^{bio}_{Ti} + T(K)(280{\cdot}306X^{bio}_{Fe} - 17{\cdot}396X^{bio}_{Mg} \\ &\quad - 280{\cdot}306X^{bio}_{Al} - 370{\cdot}39X^{bio}_{Ti}). \end{aligned} \quad (13)$$

Regression models of the GBPQ barometry

Inserting equations (5–8), (12) and (13) into equations (3) and (4), we obtained the following two pressure-dependent regression models of the GBPQ barometry:

$$\begin{aligned}P(1)(\text{bars}) = {} & 1 - \Delta_1 H^0/\Delta_1 V^0 + T(\text{K})(\Delta_1 S^0/\Delta_1 V^0) \\ & + 3(X_{\text{Fe}}^{\text{bio}} + X_{\text{Mg}}^{\text{bio}} - X_{\text{Al}}^{\text{bio}})(W_{\text{MgAl}}^{\text{bio}}/\Delta_1 V^0) \\ & + 3X_{\text{Ti}}^{\text{bio}}[(W_{\text{AlTi}}^{\text{bio}} - W_{\text{MgTi}}^{\text{bio}})/\Delta_1 V^0] \\ & + (1/\Delta_1 V^0)[T(\text{K})(-R\ln K_{(1)}^{\text{ideal}} - 6\text{Fa} + \text{Mga} \\ & + 2\text{Caa} - 788{\cdot}73X_{\text{Fe}}^{\text{bio}}) \\ & + P(-6\text{Fb} + \text{Mgb} + 2\text{Cab}) - 6\text{Fc} + \text{Mgc} \\ & + 2\text{Cac} + 667683{\cdot}0X_{\text{Fe}}^{\text{bio}}] \end{aligned} \quad (14)$$

and

$$\begin{aligned}P(2)(\text{bars}) = {} & 1 - \Delta_2 H^0/\Delta_2 V^0 + T(\text{K})(\Delta_2 S^0/\Delta_2 V^0) \\ & + 3(X_{\text{Fe}}^{\text{bio}} + X_{\text{Mg}}^{\text{bio}} - X_{\text{Al}}^{\text{bio}})(W_{\text{MgAl}}^{\text{bio}}/\Delta_2 V^0) \\ & + 3X_{\text{Ti}}^{\text{bio}}[(W_{\text{AlTi}}^{\text{bio}} - W_{\text{MgTi}}^{\text{bio}})/\Delta_2 V^0] \\ & + (1/\Delta_2 V^0)[T(\text{K})(-R\ln K_{(2)}^{\text{ideal}} - 6\text{Fa} \\ & + \text{Fea} + 2\text{Caa} - 840{\cdot}918X_{\text{Fe}}^{\text{bio}} \\ & + 52{\cdot}188X_{\text{Mg}}^{\text{bio}} + 840{\cdot}918X_{\text{Al}}^{\text{bio}} \\ & + 1111{\cdot}17X_{\text{Ti}}^{\text{bio}}) + P(-6\text{Fb} + \text{Feb} + 2\text{Cab}) \\ & - 6\text{Fc} + \text{Fec} + 2\text{Cac} + 736677{\cdot}0X_{\text{Fe}}^{\text{bio}} \\ & - 68994{\cdot}0X_{\text{Mg}}^{\text{bio}} - 736677{\cdot}0X_{\text{Al}}^{\text{bio}} \\ & - 932970{\cdot}0X_{\text{Ti}}^{\text{bio}}] \end{aligned} \quad (15)$$

in which the enthalpy-, entropy-, volume- and Margules parameter-related items are constants to be determined through regression.

METAPELITIC SAMPLES

In empirical calibration natural rock samples are necessary. Sample selection is based on the criteria of Hoisch (1990, 1991), and the samples for calibration must fit the following: (1) there is clear description of textural equilibria among garnet, biotite, plagioclase, quartz and aluminosilicate in the literature; (2) the samples did not undergo retrogressive metamorphism; (3) there are detailed and high-quality electron microprobe analyses of the minerals involved, at least SiO_2, TiO_2, Al_2O_3, FeO, MnO, MgO, CaO, Na_2O and K_2O were analysed, and the stoichiometry of the analysed minerals was confirmed; (4) if there is growth zoning in garnet, only the rim composition was used, and accordingly, only the (rim) compositions of matrix biotite and plagioclase not in contact with garnet were used. The 224 natural aluminosilicate-bearing metapelitic samples listed in Electronic Appendix A, which may be downloaded from http://www.petrology.oupjournals.org, were used to calibrate the GBPQ barometer. These samples fall in the mineral composition ranges: $X_{\text{gros}} = 3$–23% (mostly between 5 and 10%), $X_{\text{an}} = 17$–93% (mostly between 20 and 40%), and $X_{\text{Al}}^{\text{bio}} = 3$–$32\%$ (mostly between 10 and 20%). Among these 224 samples, 15 contain only andalusite, 118 contain only sillimanite, 73 contain only kyanite, 6 contain andalusite + sillimanite, and 12 contain sillimanite + kyanite. Simultaneously determined garnet–biotite temperatures (Holdaway, 2000) and GASP pressures (Holdaway, 2001) of these assemblages generally do not violate the stability field of the aluminosilicate minerals (Fig. 1a). The P–T range of these samples estimated from the garnet–biotite thermometer and GASP barometer is 1·0–11·4 kbar and 515–878°C. One sillimanite-bearing rock (sample 699-87, Neogi *et al.*, 1998) has the extremely high temperature of 878°C.

For anhydrous minerals, through charge balance and ideal formulae, methods have been developed to estimate ferric iron contents (e.g. Droop, 1987). However, such methods are probably not valid for hydrous minerals, especially those with partially vacant cation sites and variable H_2O contents, e.g. amphiboles and micas (Krogh & Raheim, 1978). After analysing 52 metapelitic biotite samples of NW Maine, USA, using Mössbauer spectroscopy, Dyar (1990) and Guidotti & Dyar (1991) found that the Fe^{3+}/Fe_{tot} mole ratio of biotite varies between 0·05 and 0·46 (mostly between 0·1 and 0·16), and the average molar percentage of ferric iron is 13·35%. This suggests that Holdaway's (2000, 2001) assumption of the mole percentage of 11·6% ferric iron in pelitic biotite is reasonable.

To satisfy internal thermodynamic consistency with the Holdaway (2000, 2001) calibrations, it is assumed that there is 3 mol % ferric iron in garnet, and 11·6 mol % ferric iron in biotite for the ilmenite-bearing natural metapelites (Electronic Appendix A) from the literature used to calibrate the GBPQ barometry. For the small number of magnetite-bearing natural metapelite samples, a 20 mol % ferric iron content is assumed.

Recently, the effects of calcium content in garnet and plagioclase on the GASP barometer have been stressed. The GASP barometer is valid for higher anorthite content in plagioclase and higher grossular content in garnet (Todd, 1998; Holdaway, 2001). In many metapelites, the mole fraction of grossular in garnet is less than 10%, and in typical metapelites the anorthite component of plagioclase is commonly less than 30% (Todd, 1998). After theoretical modelling and analyses of natural metapelites, Todd (1998) found that the difference in pressure determination between GASP barometry and non-Ca-bearing equilibria (Berman, 1991) is highly variable, and can be as high as >3 kbar when the grossular mole fraction is <10% and anorthite mole fraction is <30%. Todd concluded that the GASP barometer should be used with great caution when the product $X_{\text{an}} \cdot X_{\text{gros}}$ is <0·05.

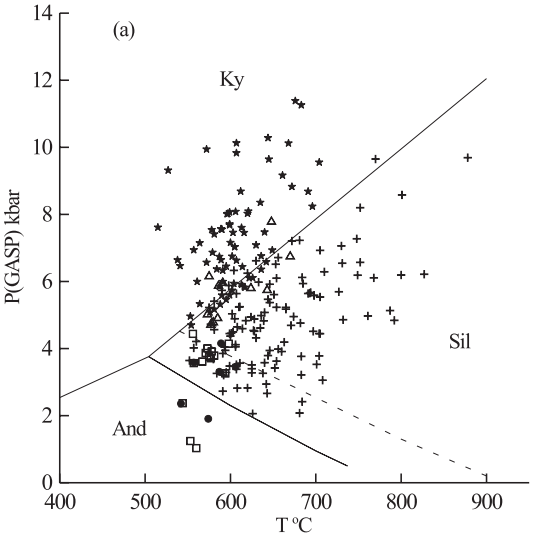

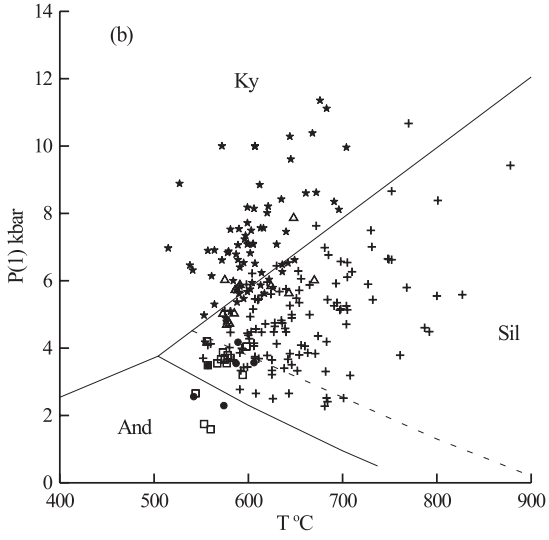

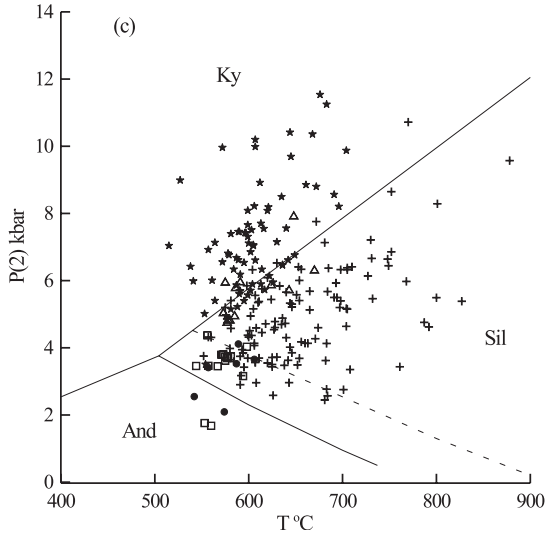

Table 2: Regressed parameters ($\pm 2\sigma$) in calibrating the GBPQ barometry

(a) *GBPQ barometry model reaction (1)*

$(\Delta_1 H^0/\Delta_1 V^0) = 24451{\cdot}7\ (\pm 537{\cdot}592)$ bar

$(\Delta_1 S^0/\Delta_1 V^0) = 40{\cdot}238\ (\pm 0{\cdot}659)$ bar/K

$(W^{bio}_{MgAl}/\Delta_1 V^0) = 1724{\cdot}620\ (\pm 157{\cdot}895)$ bar

$[(W^{bio}_{AlTi} - W^{bio}_{MgTi})/\Delta_1 V^0] = 2131{\cdot}139\ (\pm 501{\cdot}831)$ bar

$(1/\Delta_1 V^0) = 0{\cdot}081\ (\pm 0{\cdot}001)$ bar/J

The correlation coefficient $R = 0{\cdot}98$

(b) *GBPQ barometry model reaction (2)*

$(\Delta_2 H^0/\Delta_2 V^0) = 19872{\cdot}0\ (\pm 454{\cdot}875)$ bar

$(\Delta_2 S^0/\Delta_2 V^0) = 30{\cdot}750\ (\pm 0{\cdot}528)$ bar/K

$(W^{bio}_{MgAl}/\Delta_2 V^0) = 2317{\cdot}205\ (\pm 143{\cdot}210)$ bar

$[(W^{bio}_{AlTi} - W^{bio}_{MgTi})/\Delta_2 V^0] = 288{\cdot}781\ (\pm 443{\cdot}288)$ bar

$(1/\Delta_2 V^0) = 0{\cdot}081\ (\pm 0{\cdot}001)$ bar/J

The correlation coefficient $R = 0{\cdot}99$

Furthermore, after refinement of the GASP barometer, Holdaway (2001) found that GASP can be used for $X_{an} > 17\%$ and $X_{gros} > 3\%$. In this study, for the 224 natural aluminosilicate-bearing metapelites (Electronic Appendix A) used to calibrate the GBPQ barometry, the composition criteria of $X_{an} > 17\%$ and $X_{gros} > 3\%$ are guaranteed.

CALIBRATION

The mineral chemical data for the 224 metapelitic samples in Electronic Appendix A were inserted into equations (14) and (15), and the two sets of overdetermined pressure-dependent equations were subjected to multiple regression analyses to obtain parameters that minimized the sum of squares of residuals in pressure. Through nonlinear iterative regressions, the unknowns in equations (14) and (15) were obtained and are listed in Table 2. The regressions assumed equal weights for all samples.

Substituting the regressed parameters (Table 2) into equations (14) and (15) and rearranging the equations, we obtained respectively the GBPQ $P(1)$ barometry

Fig. 1. P–T plot of the 224 aluminosilicate-bearing pelitic samples (Electronic Appendix A) used in calibrating the GBPQ barometer. Continuous lines represent the aluminosilicate equilibria of Holdaway & Mukhopadhyay (1993); the dashed line represents the andalusite = sillimanite equilibrium of Pattison (1992). Temperatures were determined using the garnet–biotite thermometer of Holdaway (2000). □, samples containing only andalusite; ●, samples containing andalusite and sillimanite; +, samples containing only sillimanite; △, samples containing kyanite and sillimanite; ⋆, samples containing only kyanite. (a) Pressures determined by the GASP barometer (Holdaway, 2001). (b) Pressures determined by the GBPQ $P(1)$ barometer. (c) Pressures determined by the GBPQ $P(2)$ barometer.

formula as

$$P(1)(\text{bars})[1-0{\cdot}081(-6\text{Fb}+\text{Mgb}+2\text{Cab})] = -24450{\cdot}7+40{\cdot}238T(\text{K})+59256{\cdot}2X_{\text{Fe}}^{\text{bio}} +5173{\cdot}9(X_{\text{Mg}}^{\text{bio}}-X_{\text{Al}}^{\text{bio}})+6393{\cdot}4X_{\text{Ti}}^{\text{bio}} +0{\cdot}081[T(\text{K})(-R\ \ln K_{(1)}^{\text{ideal}}-6\text{Fa}+\text{Mga}+2\text{Caa} -788{\cdot}7X_{\text{Fe}}^{\text{bio}})-6\text{Fc}+\text{Mgc}+2\text{Cac}] \quad (16)$$

and the GBPQ $P(2)$ barometry formula as

$$P(2)(\text{bars})[1-0{\cdot}081(-6\text{Fb}+\text{Feb}+2\text{Cab})] =-19871{\cdot}0+30{\cdot}75T(\text{K})+66622{\cdot}5(X_{\text{Fe}}^{\text{bio}}-X_{\text{Al}}^{\text{bio}}) +1363{\cdot}1X_{\text{Mg}}^{\text{bio}}-74704{\cdot}2X_{\text{Ti}}^{\text{bio}}+0{\cdot}081 \times[T(\text{K})(-R\ln K_{(2)}^{\text{ideal}}-6\text{Fa}+\text{Fea}+2\text{Caa}-840{\cdot}9X_{\text{Fe}}^{\text{bio}} +52{\cdot}2X_{\text{Mg}}^{\text{bio}}+840{\cdot}9X_{\text{Al}}^{\text{bio}}+1111{\cdot}2X_{\text{Ti}}^{\text{bio}}) -6\text{Fc}+\text{Fec}+2\text{Cac}]. \quad (17)$$

The resulting GBPQ $P(1)$ and $P(2)$ barometry reproduced the input GASP pressures well within error of $\pm 1{\cdot}0$ kbar (mostly within $\pm 0{\cdot}5$ kbar), and the barometers are in excellent 1:1 linear accordance (Fig. 2a–c). Furthermore, the resulting two GBPQ barometry formulae put nearly every sample included in the calibration in the stability field of the aluminosilicate that it bears (Fig. 1b and c).

APPLICATIONS OF THE GBPQ GEOBAROMETRY

Aluminosilicate-bearing rocks

The 89 aluminosilicate-bearing samples listed in Electronic Appendix B were not used in calibrating the GBPQ barometry and, therefore, may be used as independent criteria to test the applicability of the barometry. The GASP and GBPQ pressures of these samples are in excellent 1:1 linear correlation with each other (Electronic Appendix B, Fig. 2d–f), and the GBPQ pressures of these rocks do not violate the stability field of the aluminosilicates the samples contain (Fig. 4b and c). This suggests that the GBPQ barometry is valid for the aluminosilicate-bearing metapelites. It should be pointed out that one kyanite-bearing sample, Mz80, from within the Austroalpine basement units in the eastern area of the Tauern Window, Austria (Faryad & Hoinkes, 2003), yielded a garnet–biotite temperature of 774°C and a GASP pressure of 18·065 kbar, and GBPQ $P(1)$ pressure of 18·197 kbar or GBPQ $P(2)$ pressure of 18·495 kbar (Electronic Appendix B, Fig. 2d–f). However, such high-pressure rocks are scarce; therefore, at present, we are not sufficiently confident to conclude that the GBPQ barometry may be safely applied to pressures higher than 11·4 kbar.

The P–T slopes of the GBPQ and GASP barometers are nearly identical, as indicated by two randomly picked metapelites (Fig. 3). This suggests that the two barometers have the same temperature dependence.

Aluminosilicate-free rocks

We may compare the GBPQ pressures with those computed by other barometers for the aluminosilicate-free metapelites to test the applicability of the GBPQ barometry to aluminosilicate-free metapelites. Boyle & Westhead (1992) reported data for aluminosilicate-free metapelites from the Furulund Group, Sulitjelma, Scandinavian Caledonides, and some of these rocks contain hornblende. Simultaneously applying the garnet–biotite thermometer (Holdaway, 2000) and the GBPQ barometry to these rocks yielded temperatures of 572–622°C and pressures of 7·92–10·80 kbar, whereas the garnet–hornblende–plagioclase–quartz (GHPQ) barometry (Dale *et al.*, 2000) gave pressures of 8·10–10·57 kbar; the GBPQ $P(1)$, GBPQ $P(2)$ and GHPQ pressures are in good agreement within $\pm 1{\cdot}0$ kbar (Table 3, Fig. 5).

Other hornblende-bearing and aluminosilicate-free metapelitic rocks (Burton *et al.*, 1989; Kamber, 1993), also give concordant GBPQ and GHPQ pressures (Table 3, Fig. 5).

We collated data from the literature for an additional 160 metapelitic samples without aluminosilicate or hornblende, which yielded temperatures and pressures in the range 448–737°C and 2·15–12·35 kbar. No information was available to confirm the validity of the GBPQ barometry; however, the GBPQ $P(1)$ and $P(2)$ pressures are identical within error of $\pm 0{\cdot}5$ kbar, suggesting that thermal equilibria may have been reached, and that the equivalency of these two formulae is valid. For simplicity, these data were not included in this paper.

Applications to rocks within limited geographical areas

In general, regional metamorphic rocks within a very limited geographical area, without post-metamorphic structural discontinuity, should have equilibrated under constant pressure; this phenomenon is an independent criterion in testing the applicability of a barometer.

Gordon *et al.* (1991) collected six aluminosilicate-absent metapelitic rocks within 800 m of each other that straddle the sillimanite–biotite isograd in the File Lake area, Manitoba, Canada (Electronic Appendix B). Among these samples, one (20-27) contains sillimanite but not garnet, two (2026-2 and 2040-2) contain sillimanite, and

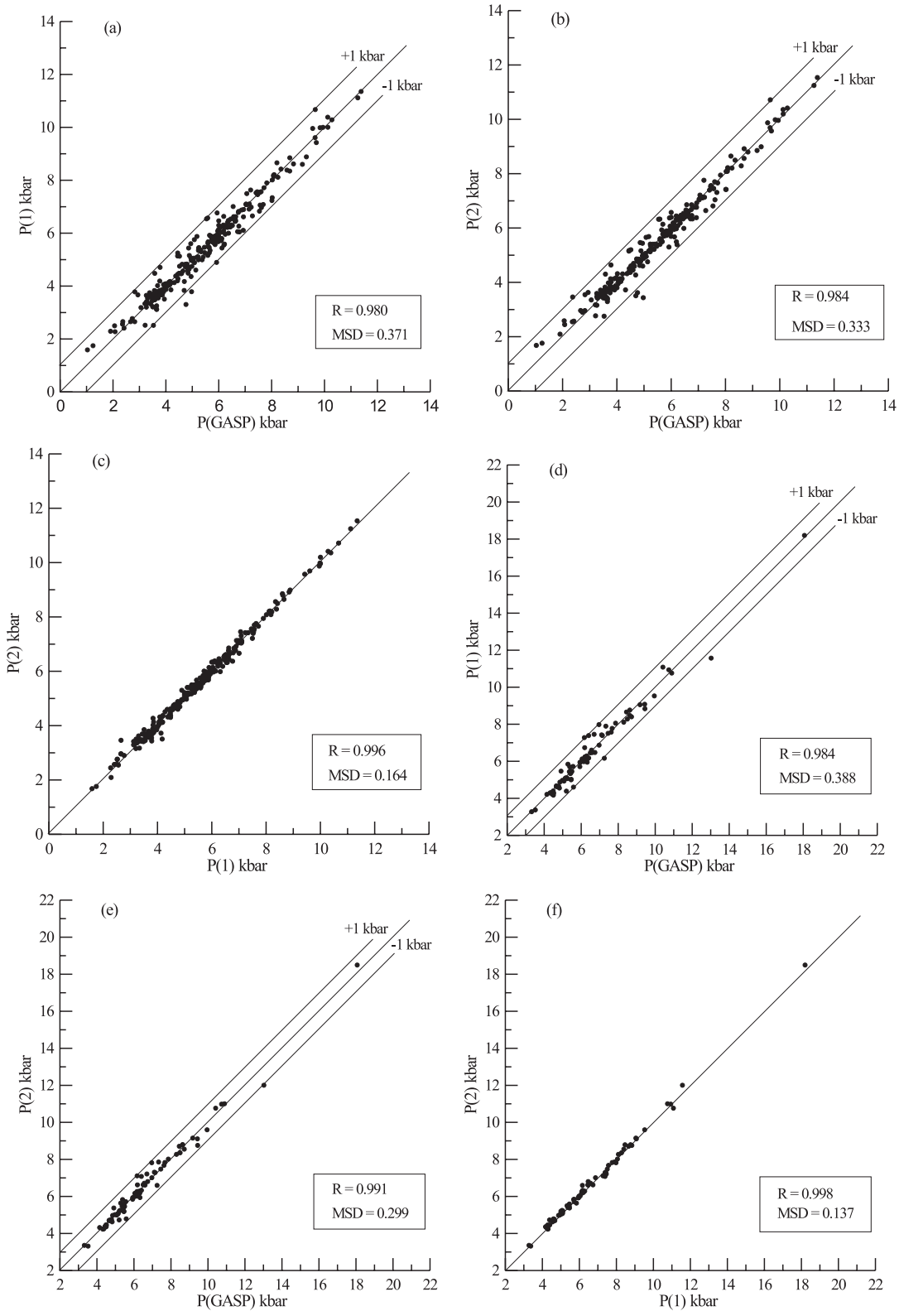

Fig. 2. Comparison of calculated pressures using the GASP, GBPQ $P(1)$ and GBPQ $P(2)$ barometers. The 224 aluminosilicate-bearing pelitic samples (Electronic Appendix A) used in calibrating the GBPQ barometry are plotted in (a)–(c), and the 89 aluminosilicate-bearing pelitic samples (Electronic Appendix B) not included in calibrating the GBPQ barometry are plotted in (d)–(f).

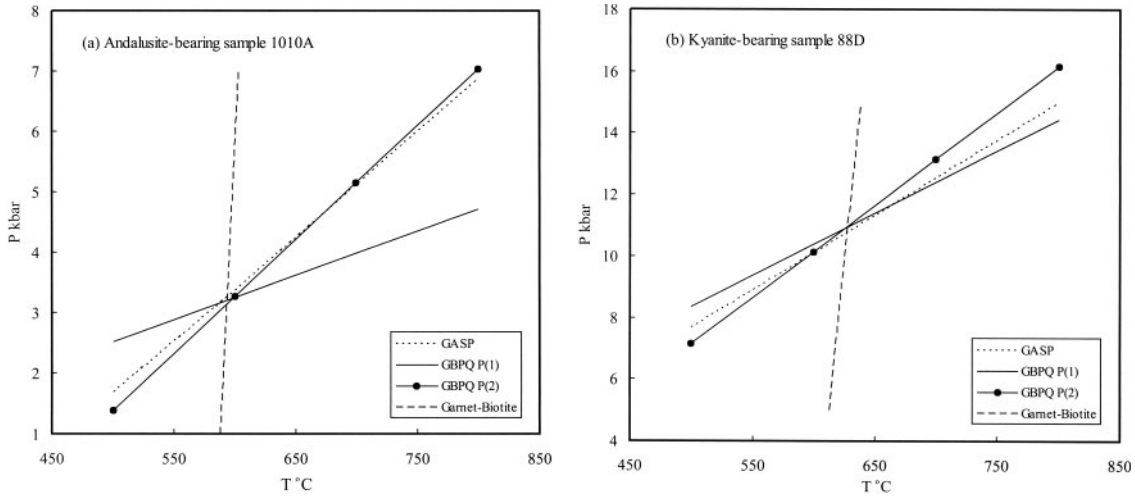

Fig. 3. *P–T* determination of (a) the andalusite-bearing metapelite 1010A (Ferry, 1980) and (b) the kyanite-bearing metapelite 88D (Himmelberg *et al.*, 1991). Sample 1010A (Electronic Appendix A) was included in the calibration of the GBPQ barometry, whereas sample 88D (Electronic Appendix B) was not included in the calibration.

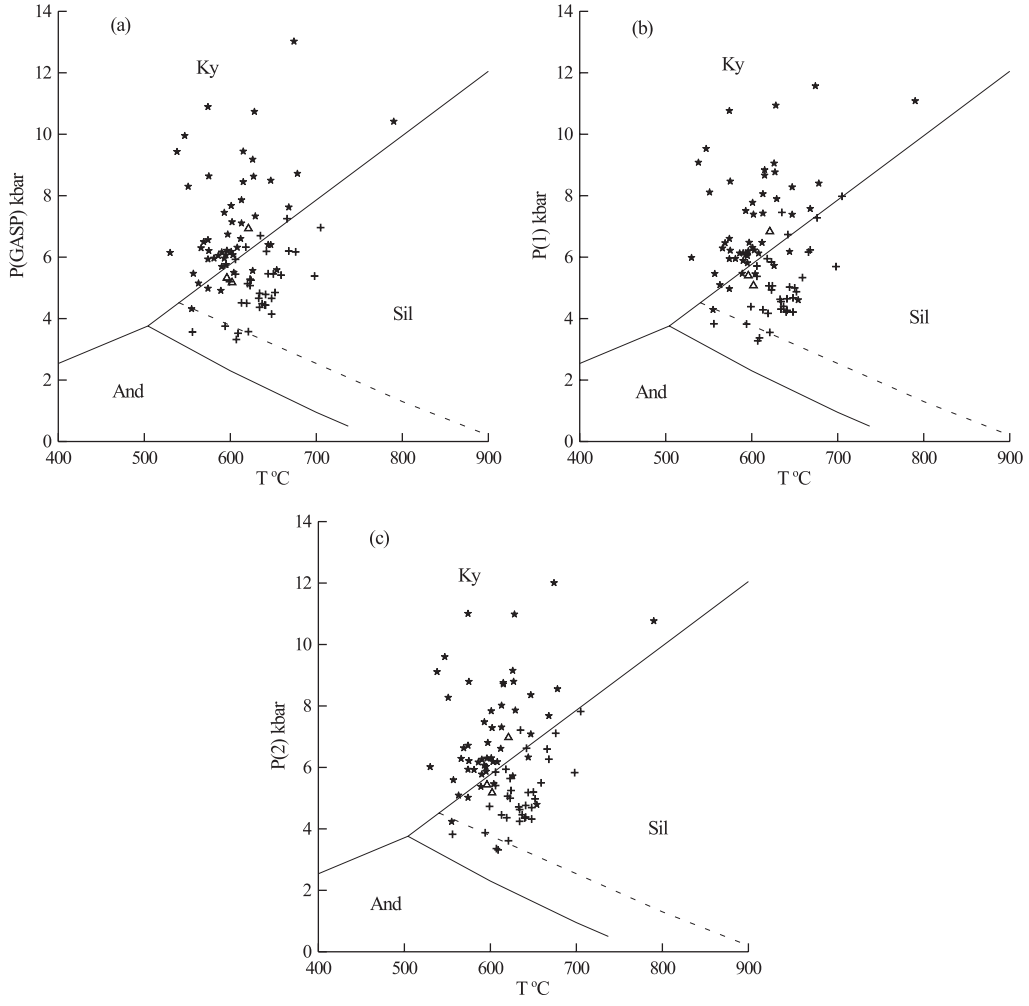

Fig. 4. *P–T* plot of the 88 aluminosilicate-bearing pelitic samples (Electronic Appendix B) not included in calibrating the GBPQ barometry. The kyanite-bearing sample Mz80 (Faryad & Hoinkes, 2003) was not plotted. Continuous lines represent the aluminosilicate equilibria of Holdaway & Mukhopadhyay (1993); the dashed line represents the andalusite = sillimanite equilibrium of Pattison (1992). Temperatures were determined using the garnet–biotite thermometer of Holdaway (2000). Symbols are as in Fig. 1. (a) Pressures determined by the GASP barometer (Holdaway, 2001). (b) Pressures determined by the GBPQ *P*(1) barometer. (c) Pressures determined by the GBPQ *P*(2) barometer.

Table 3: Application of the GBPQ barometry to aluminosilicate-free metapelites

Reference	Sample	*T*(gb) (°C)	*P*(1) (kbar)	*P*(2) (kbar)	*P*(GHPQ) (kbar)
Boyle & Westhead	70891	618	10·143	10·202	10·572
(1992)	70893	622	10·194	10·276	10·572
	75176	584	10·266	10·399	9·782
	75772	599	9·865	9·926	9·973
	70894	608	10·652	10·796	9·735
	70895	590	9·876	9·953	9·135
	70899	622	9·110	9·201	9·693
	70901	572	8·146	8·189	8·475
	69305	572	7·966	7·947	8·312
	69291	598	7·958	7·921	8·153
	70878	574	9·743	9·961	8·576
	70954	575	8·689	8·752	8·103
Burton *et al.* (1989)	268Cr	591	8·351	8·483	8·261
Kamber (1993)	BGR2	500	6·201	6·420	6·249
Koroknai *et al.* (1999)	BK2	595	10·101	12·271	
	BK10	588	11·117	11·468	
	BK11	576	10·278	10·524	
	BK12	609	10·653	10·783	
Selverstone & Spear	A6r	549	7·163	7·060	
(1985)	17Ar	561	6·628	6·743	
	27Br	577	7·571	7·404	
Droop *et al.* (2003)	Dun1*	616	3·422	3·362	
	BHQ5	660	3·295	3·108	

T(gb), garnet—biotite temperature (Holdaway, 2000); *P*(1) and P(2), GBPQ *P*(1) and *P*(2) pressure, respectively. *P*(GHPQ), garnet—hornblende—plagioclase—quartz pressure (Dale *et al.*, 2000).
*Sample Dun1 contains sillimanite.

the other three (1001, 2025A and 2038) contain garnet but no aluminosilicate. The garnet–biotite thermometer (Holdaway, 2000) and GASP barometer (Holdaway, 2001) yielded metamorphic conditions of 556°C and 3·56 kbar and 594°C and 3·75 kbar for sillimanite-bearing samples 2026-2 and 2040-2, respectively. Therefore it is reasonable to infer that the rocks were metamorphosed at a common pressure of 3·65 kbar. Simultaneously applying the garnet–biotite thermometer (Holdaway, 2000) and the GBPQ barometry to the metapelites yielded temperatures of 549–573°C and pressures of 3·12–3·37 kbar for the three aluminosilicate-absent samples, and 3·82–3·88 kbar for the two sillimanite-bearing samples. These pressures are nearly identical to the assumed constant pressure of 3·65 kbar, within error. These samples were not included in the calibration of the GBPQ barometry.

Two metamorphic mineral assemblages, a staurolite-bearing assemblage (staurolite + garnet + biotite + quartz + muscovite + plagioclase + ilmenite + magnetite), and a staurolite–kyanite-bearing assemblage (kyanite + staurolite + garnet + biotite + quartz + muscovite + plagioclase + ilmenite + rutile + pyrrhotite), are randomly distributed along a 0·5 km long exposure at the Hunt Valley Mall, north of Baltimore, Maryland, USA (Lang, 1991). Of 13 samples, six contain kyanite, five are aluminosilicate-free and calcium-deficient, and two are aluminosilicate-free but not calcium-deficient (HV114.2 and HV116.2). Application of the garnet–biotite thermometer (Holdaway, 2000) and GASP barometer (Holdaway, 2001) to the kyanite-bearing samples yielded uniform metamorphic conditions of 590–603°C and 5·69–6·22 kbar (Electronic Appendix B). It is reasonably assumed that a uniform pressure of 6·0 kbar had been reached. Lang (1991) attributed the *P–T* uniformity and mineral assemblage difference to differences in the bulk-rock composition of the two assemblages. Simultaneously applying the garnet–biotite thermometer (Holdaway, 2000) and the GBPQ barometry to the metapelites yielded temperatures of 589–603°C and pressures of 6·30–6·57 kbar for the two aluminosilicate-absent samples (HV114.2 and HV116.2), and 5·78–6·31 kbar for the six kyanite-bearing samples. These pressures are nearly identical to the uniform pressure of 6·0 kbar, within error. These samples were also not included in the calibration of the GBPQ barometry.

Other examples of closely associated rocks provide additional opportunities to test the applicability of the GBPQ barometry. Four aluminosilicate-free, metapelitic rocks that were 1·5 km apart (BK2, BK10, BK11 and BK12) were sampled from the Bundschuh nappe, eastern Alps (Koroknai *et al.*, 1999). Simultaneously applying the garnet–biotite thermometry (Holdaway, 2000) and the GBPQ barometry yielded temperatures of 576–609°C and GBPQ pressures of 10·28–11·47 kbar, respectively, suggesting nearly a uniform pressure of metamorphism, within error. The *P*(1) and *P*(2) formulae gave identical pressures for every sample (Table 3, Fig. 5c).

Three aluminosilicate-absent metapelitic rocks that were 1 km apart (6Ar, 17Ar and 27Br) were sampled from the SW Tauern Window, eastern Alps (Selverstone & Spear, 1985). Simultaneously applying the garnet–biotite thermometer (Holdaway, 2000) and the GBPQ barometry yielded temperatures between 549 and 577°C and pressures between 6·63 and 7·57 kbar (Table 3, Fig. 5c), suggesting a uniform pressure of 7·1 kbar, within error; the *P*(1) and *P*(2) formulae gave identical pressures for each sample.

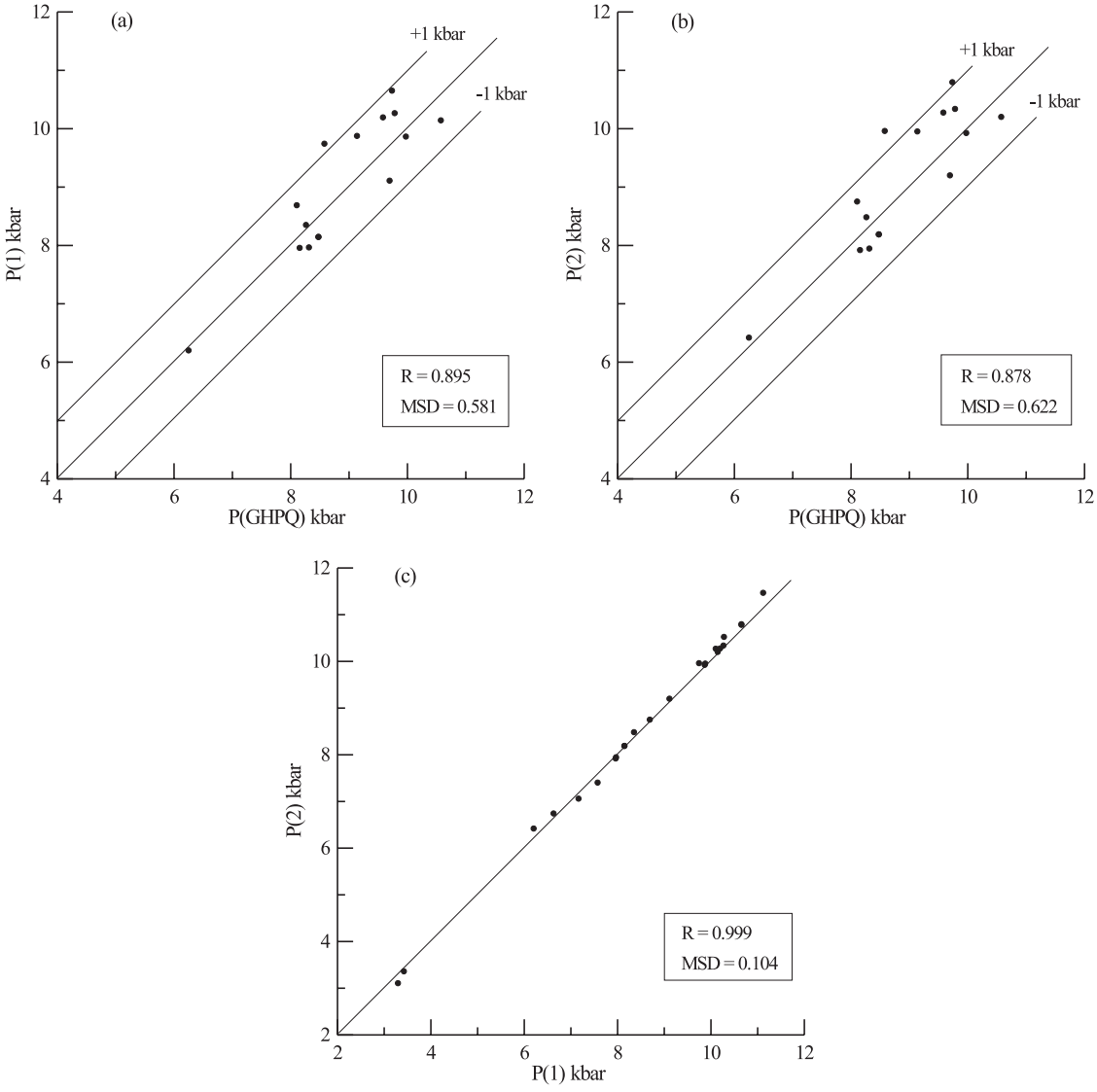

Fig. 5. Comparison of the calculated pressures using the GBPQ *P*(1), GBPQ *P*(2) barometer and the garnet–hornblende–plagioclase–quartz (GHPQ) barometer (Dale *et al.* 2000) for the aluminosilicate-free samples, including one sillimanite-bearing metapelite Dun1 (Table 3).

Rocks in contact metamorphic aureoles

Rocks that formed at thermodynamic equilibrium within a limited contact metamorphic aureole should have been metamorphosed at the same pressure. We may thus check the applicability of the GBPQ barometry by applying it to contact aureole rocks.

From Garnet Ledge, SE Alaska, two metapelitic samples from a contact aureole at the same geographical location were collected (Stowell *et al.*, 2001). The garnet–biotite thermometer (Holdaway, 2000) and GASP barometer (Holdaway, 2001) yielded temperatures and pressures of 640°C and 5·08 kbar for sample GL02 and 624°C and 4·94 kbar for sample GL03, respectively. Our GBPQ barometry yielded pressures of 5·66–5·76 kbar and 5·44–5·60 kbar for the two samples, respectively, similar to the GASP results, within error (Electronic Appendix A).

Two metapelitic hornfels, a sillimanite-bearing sample Dun1 and an aluminosilicate-free sample BHQ5, were collected from the contact aureole of the Huntly Gabbro Complex, NE Scotland (Droop *et al.*, 2003). Simultaneously applying the garnet–biotite thermometer (Holdaway, 2000) and the GASP barometer (Holdaway, 2001) to sample Dun1 yielded a temperature of 616°C and a pressure of 2·83 kbar. The GBPQ barometer yielded a pressure of 3·11–3·42 kbar for the two samples

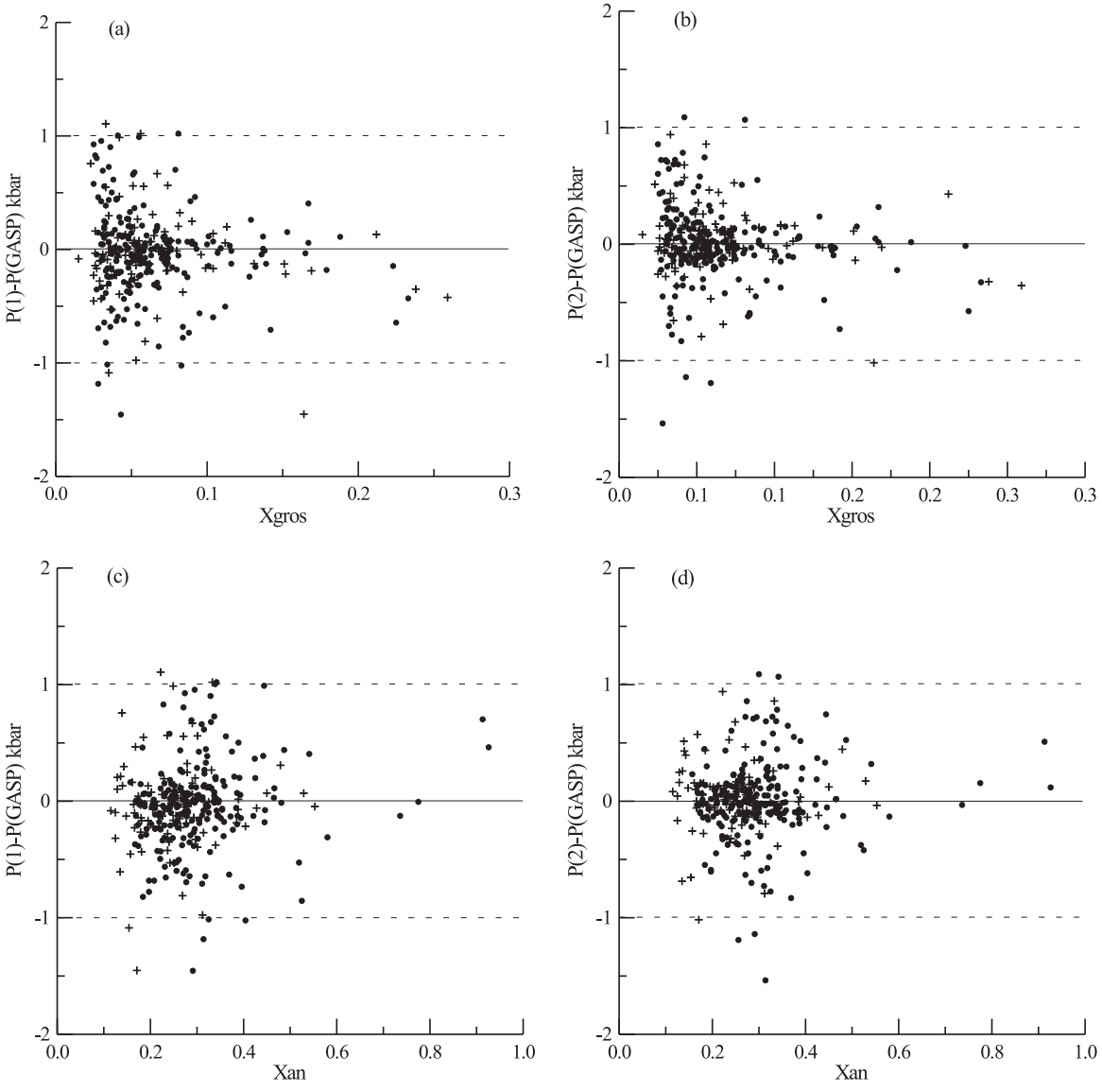

Fig. 6. The difference between GASP and GBPQ pressures as a function of the calcium content in garnet (X_{gros}; a, b) and plagioclase (X_{an}; c, d). •, the 224 aluminosilicate-bearing pelitic samples used in calibrating the GBPQ barometer; +, the 89 aluminosilicate-bearing pelitic samples not used in the calibration.

(Table 3), suggesting constant-pressure contact metamorphism.

ERROR CONSIDERATIONS

As there are no experiments to calibrate the GBPQ barometer, the absolute errors of the barometer equations cannot be evaluated. However, the excellent 1:1 relationships among the GASP and GBPQ $P(1)$ and $P(2)$ barometers (Fig. 2) suggest that the results of GBPQ barometry are in excellent agreement with the GASP barometer within error of ±1·0 kbar (mostly within ±0·5 kbar), at least in the P–T range 1·0–11·4 kbar and 515–878°C.

Random errors associated with application of the barometers come from uncertainties associated with the input temperature, electron microprobe analytical errors in the concentrations of relevant elements in garnet, plagioclase and biotite, and uncertainty in the activity models. Much of the error in the activity models is expected to be compensated for by the use of the same activity models in the garnet–biotite thermometer (Holdaway, 2000) and GASP barometer (Holdaway, 2001). However, any detailed analysis of pressure errors by propagation of individual errors is a nearly impossible task with the present barometry because of the complex formalism. Assuming that the

most important sources of error come from errors in the input temperature, and analytical errors in the concentration of Ca in garnet and plagioclase, and Al in biotite, we may estimate the approximate uncertainty of the GBPQ barometer through numerical modelling, neglecting the correlation coefficients between these sources of error.

On the basis of the sample dataset in Electronic Appendices A and B and Table 3, through numerical modelling, we observe that: (1) an input temperature error of ±50°C will introduce a pressure error of ±0·02–1·2 kbar (mostly between ±0·2 and ±0·8 kbar), and ±0·02–1·6 kbar (mostly between ±0·6 and ±1·4 kbar) for the GBPQ $P(1)$ and $P(2)$ barometers, respectively; (2) assuming an analytical error of ±5% for the Ca content in plagioclase, the resulting uncertainty in the GBPQ pressures will be ±0·01–0·25 kbar (mostly between ±0·05 and ±0·15 kbar) for both $P(1)$ and $P(2)$; (3) assuming an analytical error of ±5% for the Ca content in garnet, the resulting uncertainty in the GBPQ pressures will be ±0·12–0·17 kbar (mostly between ±0·10 and ±0·20 kbar) for both $P(1)$ and $P(2)$; (4) assuming an analytical error of ±5% for the Al content in biotite, the resulting uncertainty in the GBPQ pressures will be ±0·001–0·102 kbar (mostly between ±0·01 and ±0·05 kbar) for $P(1)$ and ±0·004–0·15 kbar (mostly between ±0·01 and ±0·06 kbar) for $P(2)$, respectively. Simply summing the errors from the above sources for all the samples and then averaging the total value based on the total number of samples, we predict that the random error is ±1·2 kbar for the GBPQ barometry. However, it should be noted that this value is somewhat arbitrary. Nevertheless, by comparing the GASP and GBPQ pressures, it appears that this random error may be approximately correct.

The difference between the GASP and GBPQ pressures becomes somewhat greater when X_{gros} is <0·05 than when X_{gros} is >0·05 (Fig. 6a and b); the pressure difference also becomes slightly greater when X_{an} is <0·25 than when X_{an} is >0·25 (Fig. 6c and d). This suggests that the GBPQ barometry may be most inaccurate for samples with low-Ca garnet (especially when X_{gros} is <0·05) and low-Ca plagioclase. However, the application of the GBPQ barometer in the composition range X_{gros} >0·03 and X_{an} >0·17 seems promising for most metapelites. The difference between the GASP and GBPQ pressures seems to be relatively insensitive to the Fe/Mg ratio in both garnet and biotite.

ACKNOWLEDGEMENTS

Professor Michael J. Holdaway generously sent us his garnet–biotite thermometer and GASP barometer programs. Dr Clifford S. Todd kindly provided us with the complete Alpine mineral dataset. Reviews by Michael Holdaway and Ian Fitzsimons, and the editorial work of Geoffrey Clarke, have greatly improved the quality of the original manuscript. This work was supported by the National Natural Science Foundation of China (grant numbers 40002017, 40174027 and 40172065) and a Presidential Fund from The Chinese Academy of Sciences.

SUPPLEMENTARY DATA

Supplementary data for this paper are availabe on *Journal of Petrology* online.

REFERENCES

Barboza, S. A. & Bergantz, G. W. (2000). Metamorphism and anatexis in the mafic complex contact aureole, Ivrea Zone, Northern Italy. *Journal of Petrology* **41**, 1307–1327.

Berman, R. G. (1991). Thermobarometry using multi-equilibrium calculations: a new technique, with petrological applications. *Canadian Mineralogist* **29**, 833–855.

Berman, R. G. & Aranovich, L. Ya. (1996). Optimized standard state and solution properties of minerals. I. Calibration for olivine, orthopyroxene, cordierite, garnet, and ilmenite in the system FeO–MgO–CaO–Al_2O_3–TiO_2–SiO_2. *Contributions to Mineralogy and Petrology* **126**, 1–24.

Boyle, A. P. & Westhead, R. K. (1992). Metamorphic peak geothermobarometry in the Furulund Group, Sulitjelma, Scandinavian Caledonides: implications for uplift. *Journal of Metamorphic Geology* **10**, 615–626.

Burton, K. W., Boyle, A. P., Kirk, W. L. & Mason, R. (1989). Pressure, temperature and structural evolution of the Sulitjelma fold-nappe, central Scandinavian Caledonides. In: Daly, J. S., Cliff, R. A. & Yardley, B. W. D. (eds) *Evolution of Metamorphic Belts. Geological Society, London, Special Publications* **43**, 391–411.

Dale, J., Holland, T. & Powell, R. (2000). Hornblende–garnet–plagioclase thermobarometry: a natural assemblage calibration of the thermodynamics of hornblende. *Contributions to Mineralogy and Petrology* **140**, 353–362.

Delor, C. P., Burg, J. P. & Leyreloup, A. F. (1984). Staurolite producing reactions and geothermobarometry of a high pressure thermal aureole in the French Massif Central. *Journal of Metamorphic Geology* **2**, 55–72.

Droop, G. T. R. (1987). A general equation for estimating Fe^{3+} concentrations in ferromagnesian silicates and oxides from microprobe analyses, using stoichiometric criteria. *Mineralogical Magazine* **51**, 431–435.

Droop, G. T. R., Clemens, J. D. & Dalrymple, D. J. (2003). Processes and conditions during contact anatexis, melt escape and restite formation: the Huntly Gabbro Complex, NE Scotland. *Journal of Petrology* **44**, 995–1029.

Dyar, M. D. (1990). Mössbauer spectra of biotite from metapelites. *American Mineralogist* **75**, 656–666.

Engi, M., Todd, C. S. & Schmatz, D. R. (1995). Tertiary metamorphic conditions in the eastern Lepontine Alps. *Schweizerische Mineralogische und Petrographische Mitteilungen* **75**, 347–369.

Faryad, S. W. & Hoinkes, G. (2003). *P–T* gradient of Eo-Alpine metamorphism within the Austroalpine basement units east of the Tauern Window (Austria). *Mineralogy and Petrology* **77**, 129–159.

Ferry, J. M. (1980). A comparative study of geothermometers and geobarometers in pelitic schists from south–central Maine. *American Mineralogist* **65**, 720–732.

Ferry, J. M. & Spear, F. S. (1978). Experimental calibration of the partitioning of Fe and Mg between biotite and garnet. *Contributions to Mineralogy and Petrology* **66**, 113–117.

Fuhrman, M. L. & Lindsley, D. H. (1988). Ternary-feldspar modeling and thermometry. *American Mineralogist* **73**, 201–215.

Ganguly, J., Cheng, W. & Tirone, M. (1996). Thermodynamics of aluminosilicate garnet solid solution: new experimental data, an optimized model, and thermodynamic applications. *Contributions to Mineralogy and Petrology* **126**, 137–151.

Gasparik, T. (1984). Experimental study of the subsolidus phase relations and mixing properties of pyroxene in the system CaO–Al_2O_3–SiO_2. *Geochimica et Cosmochimica Acta* **48**, 2537–2545.

Ghent, E. D. & Stout, M. Z. (1981). Geobarometry and geothermometry of plagioclase–biotite–garnet–muscovite assemblages. *Contributions to Mineralogy and Petrology* **76**, 92–97.

Goldsmith, J. R. (1980). Melting and breakdown reactions of anorthite at high pressures and temperatures. *American Mineralogist* **65**, 272–284.

Gordon, T. M., Ghent, E. D. & Stout, M. Z. (1991). Algebraic analysis of the biotite–sillimanite isograd in the File Lake area, Manitoba. *Canadian Mineralogist* **29**, 673–686.

Guidotti, C. V. & Dyar, M. D. (1991). Ferric iron in metamorphic biotite and its petrologic and crystallochemical implications. *American Mineralogist* **76**, 161–175.

Hariya, Y. & Kennedy, G. C. (1968). Equilibrium study of anorthite under high temperature and high pressure. *American Journal of Science* **266**, 193–203.

Hays, J. F. (1966). Lime–alumina–silica. *Carnegie Institution of Washington Yearbook* **65**, 234–239.

Himmelberg, G. R., Brew, D. A. & Ford, A. B. (1991). Development of inverted metamorphic isograds in the western metamorphic belt, Juneau, Alaska. *Journal of Metamorphic Geology* **9**, 165–180.

Hodges, K. V. & Crowley, P. D. (1985). Error estimation in empirical geothermometry and geobarometry for pelitic systems. *American Mineralogist* **70**, 702–709.

Hoisch, T. D. (1990). Empirical calibration of six geobarometers for the mineral assemblage quartz + muscovite + biotite + plagioclase + garnet. *Contributions to Mineralogy and Petrology* **104**, 225–234.

Hoisch, T. D. (1991). Equilibria within the mineral assemblage quartz + muscovite + biotite + garnet + plagioclase, and implications for the mixing properties of octahedrally-coordinated cations in muscovite and biotite. *Contributions to Mineralogy and Petrology* **108**, 43–54.

Holdaway, M. J. (2000). Application of new experimental and garnet Margules data to the garnet–biotite geothermometer. *American Mineralogist* **85**, 881–892.

Holdaway, M. J. (2001). Recalibration of the GASP geobarometer in light of recent garnet and plagioclase activity models and versions of the garnet–biotite geothermometer. *American Mineralogist* **86**, 1117–1129.

Holdaway, M. J. & Mukhopadhyay, B. (1993). A re-evaluation of the stability relations of andalusite: thermochemical data and phase diagram for the aluminosilicates. *American Mineralogist* **78**, 298–315.

Holdaway, M. J., Dutrow, B. L. & Hinton, R. W. (1988). Devonian and Carboniferous metamorphism in west–central Maine: the muscovite–almandine geobarometer and the staurolite problem revised. *American Mineralogist* **73**, 20–47.

Huang, M. H., Buick, I. S. & Hou, L. W. (2003). Tectonometamorphic evolution of the eastern Tibet Plateau: evidence from the central Songpan–Garzê Orogenic Belt, Western China. *Journal of Petrology* **44**, 255–278.

Kamber, B. S. (1993). Regional metamorphism and uplift along the southern margin of the Gotthard massif; results from the Nufenenpass area. *Schweizerische Mineralogische und Petrographsche Mitteilungen* **73**, 241–257.

Koroknai, B. K., Neubauer, F. & Topa, D. (1999). Metamorphic and tectonic evolution of Australpine at the western margin of the Gurktal nappe complex, Eastern Alps. *Schweizerische Mineralogische und Petrographische Mitteilungen* **79**, 277–295.

Koziol, A. M. & Newton, R. C. (1988). Redetermination of the anorthite breakdown reaction and improvement of the plagioclase–garnet–Al_2SiO_5–quartz geobarometer. *American Mineralogist* **73**, 216–223.

Krogh, J. E. & Raheim, A. (1978). Temperature and pressure dependence of Fe–Mg partitioning between garnet and phengite, with particular reference to eclogites. *Contributions to Mineralogy and Petrology* **66**, 75–80.

Lang, H. M. (1991). Quantitative interpretation of within-outcrop variation in metamorphic assemblages in staurolite–kyanite-grade metapelites, Baltimore, Maryland. *Canadian Mineralogist* **29**, 655–671.

Lang, H. M. & Rice, J. M. (1985). Regression modelling of metamorphic reactions in metapelites, Snow Peak, Northern Idaho. *Journal of Petrology* **26**, 857–887.

McMullin, D. W. A., Berman, R. G. & Greenwood, H. J. (1991). Calibration of the SGAM thermobarometer for pelitic rocks using data from phase-equilibrium experiments and natural assemblages. *Canadian Mineralogist* **29**, 889–908.

Mezger, J. E., Chacko, T. & Erdmer, P. (2001). Metamorphism at a late Mesozoic accretionary margin: a study from the Coast Belt of the North American Cordillera. *Journal of Metamorphic Geology* **19**, 121–137.

Mukhopadhyay, B., Basu, S. & Holdaway, M. J. (1993). A discussion of Margules-type formulations for multicomponent solutions with a generalized approach. *Geochimica et Cosmochimica Acta* **57**, 277–283.

Mukhopadhyay, B., Holdaway, M. J. & Koziol, A. M. (1997). A statistical model of thermodynamic mixing properties of Ca–Mg–Fe^{2+} garnets. *American Mineralogist* **82**, 165–181.

Neogi, S., Dasgupta, S. & Fukuoka, M. (1998). High *P–T* polymetamorphism, dehydration melting, and generation of migmatites and granites in the Higher Himalayan Crystalline Complex, Sikkim, India. *Journal of Petrology* **39**, 61–99.

Pattison, D. R. M. (1992). Stability of andalusite and sillimanite and the Al_2SiO_5 triple point: constraints from the Ballachulish aureole, Scotland. *Journal of Geology* **100**, 423–446.

Perchuk, L. L. & Lavrent'eva, L. Y. (1983). Experimental investigation of exchange equilibria in the system cordierite–garnet–biotite. In: Saxena, S. K. (ed.) *Kinetics and Equilibrium in Mineral Reactions. Advances in Physical Geochemistry* **3**, 199–239.

Selverstone, J. & Spear, F. S. (1985). Metamorphic *P–T* paths from pelitic schists and greenstones from the south-west Tauern Window, Eastern Alps. *Journal of Metamorphic Geology* **3**, 439–465.

Spear, F. S., Kohn, M. J. & Paetzold, S. (1995). Petrology of the regional sillimanite zone, west–central New Hampshire, U.S.A., with implications for the development of inverted isograds. *American Mineralogist* **80**, 361–376.

Stephenson, B. J., Waters, D. J. & Searle, M. P. (2000). Inverted metamorphism and the Main Central Thrust: field relations and thermobarometric constraints from the Kishtwar Window, NW Indian Himalaya. *Journal of Metamorphic Geology* **18**, 571–590.

Stowell, H. H., Taylor, D. L., Tinkham, D., Goldberg, S. A. & Ouderkirk, K. A. (2001). Contact metamorphic *P–T–t* paths from Sm–Nd garnet ages, phase equilibria modelling and thermobarometry: Garnet Ledge, south-eastern Alaska, USA. *Journal of Metamorphic Geology* **19**, 645–660.

Swapp, S. M. & Hollister, L. S. (1991). Inverted metamorphism within the Tibetan slab of Bhutan: evidence for a tectonically transposed heat-source. *Canadian Mineralogist* **29**, 1019–1041.

Todd, C. S. (1998). Limits on the precision of geobarometry at low grossular and anorthite content. *American Mineralogist* **83**, 1161–1167.

Todd, C. S. & Engi, M. (1997). Metamorphic field gradients in the Central Alps. *Journal of Metamorphic Geology* **15**, 513–530.

REFERENCES CITED ONLY IN ELECTRONIC APPENDIX

Hoisch, T. D. (1989). A muscovite–biotite geothermometer. *American Mineralogist* **74**, 565–572.

Kalt, A., Altherr, R. & Ludwig, T. (1998) Contact metamorphism in pelitic rocks on the island of Kos (Greece, Eastern Aegean Sea): a test for the Na-in-cordierite thermometer. *Journal of Petrology* **39**, 663–688.

Rothstein, D. A. & Hoisch, T. D. (1994). Multiple intrusions and low-pressure metamorphism in the central Old Woman Mountains, south-eastern California: constraints from thermal modelling. *Journal of Metamorphic Geology* **12**, 723–734.

APPENDIX

$$\begin{aligned}\mathrm{Caa} = {} & 0{\cdot}337(X_{\mathrm{Fe}}^{\mathrm{grt}})^2 - 18{\cdot}983(X_{\mathrm{Mg}}^{\mathrm{grt}})^2 \\ & - 9{\cdot}5725(X_{\mathrm{Fe}}^{\mathrm{grt}})(X_{\mathrm{Mg}}^{\mathrm{grt}}) - 19{\cdot}34(X_{\mathrm{Fe}}^{\mathrm{grt}})(X_{\mathrm{Ca}}^{\mathrm{grt}}) \\ & - 4{\cdot}6665(X_{\mathrm{Fe}}^{\mathrm{grt}})(X_{\mathrm{Mn}}^{\mathrm{grt}}) - 25{\cdot}746(X_{\mathrm{Mg}}^{\mathrm{grt}})(X_{\mathrm{Ca}}^{\mathrm{grt}}) \\ & - 38{\cdot}938(X_{\mathrm{Mg}}^{\mathrm{grt}})(X_{\mathrm{Mn}}^{\mathrm{grt}}) + 11{\cdot}006(X_{\mathrm{Fe}}^{\mathrm{grt}})^2(X_{\mathrm{Mg}}^{\mathrm{grt}}) \\ & - 0{\cdot}674(X_{\mathrm{Fe}}^{\mathrm{grt}})^2(X_{\mathrm{Ca}}^{\mathrm{grt}}) - 11{\cdot}986(X_{\mathrm{Mg}}^{\mathrm{grt}})^2(X_{\mathrm{Fe}}^{\mathrm{grt}}) \\ & + 37{\cdot}966(X_{\mathrm{Mg}}^{\mathrm{grt}})^2(X_{\mathrm{Ca}}^{\mathrm{grt}}) + 46{\cdot}02(X_{\mathrm{Mg}}^{\mathrm{grt}})^2(X_{\mathrm{Mn}}^{\mathrm{grt}}) \\ & + 19{\cdot}34(X_{\mathrm{Ca}}^{\mathrm{grt}})^2(X_{\mathrm{Fe}}^{\mathrm{grt}}) + 25{\cdot}746(X_{\mathrm{Ca}}^{\mathrm{grt}})^2(X_{\mathrm{Mg}}^{\mathrm{grt}}) \\ & + 46{\cdot}02(X_{\mathrm{Mn}}^{\mathrm{grt}})^2(X_{\mathrm{Mg}}^{\mathrm{grt}}) + 19{\cdot}145(X_{\mathrm{Fe}}^{\mathrm{grt}})(X_{\mathrm{Mg}}^{\mathrm{grt}})(X_{\mathrm{Ca}}^{\mathrm{grt}}) \\ & + 45{\cdot}53(X_{\mathrm{Fe}}^{\mathrm{grt}})(X_{\mathrm{Mg}}^{\mathrm{grt}})(X_{\mathrm{Mn}}^{\mathrm{grt}}) \\ & + 9{\cdot}333(X_{\mathrm{Fe}}^{\mathrm{grt}})(X_{\mathrm{Ca}}^{\mathrm{grt}})(X_{\mathrm{Mn}}^{\mathrm{grt}}) \\ & + 77{\cdot}876(X_{\mathrm{Mg}}^{\mathrm{grt}})(X_{\mathrm{Ca}}^{\mathrm{grt}})(X_{\mathrm{Mn}}^{\mathrm{grt}}) \end{aligned} \quad (A1)$$

$$\begin{aligned}\mathrm{Cab} = {} & 0{\cdot}04(X_{\mathrm{Fe}}^{\mathrm{grt}})^2 + 0{\cdot}068(X_{\mathrm{Mg}}^{\mathrm{grt}})^2 + 0{\cdot}065(X_{\mathrm{Mn}}^{\mathrm{grt}})^2 \\ & - 0{\cdot}0515(X_{\mathrm{Fe}}^{\mathrm{grt}})(X_{\mathrm{Mg}}^{\mathrm{grt}}) + 0{\cdot}27(X_{\mathrm{Fe}}^{\mathrm{grt}})(X_{\mathrm{Ca}}^{\mathrm{grt}}) \\ & + 0{\cdot}1765(X_{\mathrm{Fe}}^{\mathrm{grt}})(X_{\mathrm{Mn}}^{\mathrm{grt}}) + 0{\cdot}28(X_{\mathrm{Mg}}^{\mathrm{grt}})(X_{\mathrm{Ca}}^{\mathrm{grt}}) \\ & + 0{\cdot}207(X_{\mathrm{Mg}}^{\mathrm{grt}})(X_{\mathrm{Mn}}^{\mathrm{grt}}) + 0{\cdot}13(X_{\mathrm{Ca}}^{\mathrm{grt}})(X_{\mathrm{Mn}}^{\mathrm{grt}}) \\ & - 0{\cdot}1(X_{\mathrm{Fe}}^{\mathrm{grt}})^2(X_{\mathrm{Mg}}^{\mathrm{grt}}) - 0{\cdot}08(X_{\mathrm{Fe}}^{\mathrm{grt}})^2(X_{\mathrm{Ca}}^{\mathrm{grt}}) \\ & - 0{\cdot}048(X_{\mathrm{Fe}}^{\mathrm{grt}})^2(X_{\mathrm{Mn}}^{\mathrm{grt}}) + 0{\cdot}068(X_{\mathrm{Mg}}^{\mathrm{grt}})^2(X_{\mathrm{Fe}}^{\mathrm{grt}}) \\ & - 0{\cdot}136(X_{\mathrm{Mg}}^{\mathrm{grt}})^2(X_{\mathrm{Ca}}^{\mathrm{grt}}) - 0{\cdot}076(X_{\mathrm{Mg}}^{\mathrm{grt}})^2(X_{\mathrm{Mn}}^{\mathrm{grt}}) \\ & - 0{\cdot}27(X_{\mathrm{Ca}}^{\mathrm{grt}})^2(X_{\mathrm{Fe}}^{\mathrm{grt}}) - 0{\cdot}28(X_{\mathrm{Ca}}^{\mathrm{grt}})^2(X_{\mathrm{Mg}}^{\mathrm{grt}}) \\ & - 0{\cdot}13(X_{\mathrm{Ca}}^{\mathrm{grt}})^2(X_{\mathrm{Mn}}^{\mathrm{grt}}) - 0{\cdot}048(X_{\mathrm{Mn}}^{\mathrm{grt}})^2(X_{\mathrm{Fe}}^{\mathrm{grt}}) \\ & - 0{\cdot}076(X_{\mathrm{Mn}}^{\mathrm{grt}})^2(X_{\mathrm{Mg}}^{\mathrm{grt}}) - 0{\cdot}13(X_{\mathrm{Mn}}^{\mathrm{grt}})^2(X_{\mathrm{Ca}}^{\mathrm{grt}}) \\ & + 0{\cdot}103(X_{\mathrm{Fe}}^{\mathrm{grt}})(X_{\mathrm{Mg}}^{\mathrm{grt}})(X_{\mathrm{Ca}}^{\mathrm{grt}}) - 0{\cdot}14(X_{\mathrm{Fe}}^{\mathrm{grt}})(X_{\mathrm{Mg}}^{\mathrm{grt}})(X_{\mathrm{Mn}}^{\mathrm{grt}}) \\ & - 0{\cdot}353(X_{\mathrm{Fe}}^{\mathrm{grt}})(X_{\mathrm{Ca}}^{\mathrm{grt}})(X_{\mathrm{Mn}}^{\mathrm{grt}}) - 0{\cdot}414(X_{\mathrm{Mg}}^{\mathrm{grt}})(X_{\mathrm{Ca}}^{\mathrm{grt}})(X_{\mathrm{Mn}}^{\mathrm{grt}}) \end{aligned} \quad (A2)$$

$$\begin{aligned}\mathrm{Cac} = {} & -1304{\cdot}0(X_{\mathrm{Fe}}^{\mathrm{grt}})^2 + 66114{\cdot}0(X_{\mathrm{Mg}}^{\mathrm{grt}})^2 + 1425{\cdot}0(X_{\mathrm{Mn}}^{\mathrm{grt}})^2 \\ & + 31326{\cdot}5(X_{\mathrm{Fe}}^{\mathrm{grt}})(X_{\mathrm{Mg}}^{\mathrm{grt}}) + 39864{\cdot}0(X_{\mathrm{Fe}}^{\mathrm{grt}})(X_{\mathrm{Ca}}^{\mathrm{grt}}) \\ & + 12356{\cdot}0(X_{\mathrm{Fe}}^{\mathrm{grt}})(X_{\mathrm{Mn}}^{\mathrm{grt}}) + 51518{\cdot}0(X_{\mathrm{Mg}}^{\mathrm{grt}})(X_{\mathrm{Ca}}^{\mathrm{grt}}) \\ & + 88610{\cdot}5(X_{\mathrm{Mg}}^{\mathrm{grt}})(X_{\mathrm{Mn}}^{\mathrm{grt}}) + 2850{\cdot}0(X_{\mathrm{Ca}}^{\mathrm{grt}})(X_{\mathrm{Mn}}^{\mathrm{grt}}) \\ & - 23244{\cdot}0(X_{\mathrm{Fe}}^{\mathrm{grt}})^2(X_{\mathrm{Mg}}^{\mathrm{grt}}) + 2608{\cdot}0(X_{\mathrm{Fe}}^{\mathrm{grt}})^2(X_{\mathrm{Ca}}^{\mathrm{grt}}) \\ & - 3234{\cdot}0(X_{\mathrm{Fe}}^{\mathrm{grt}})^2(X_{\mathrm{Mn}}^{\mathrm{grt}}) + 11344{\cdot}0(X_{\mathrm{Mg}}^{\mathrm{grt}})^2(X_{\mathrm{Fe}}^{\mathrm{grt}}) \\ & - 132228{\cdot}0(X_{\mathrm{Mg}}^{\mathrm{grt}})^2(X_{\mathrm{Ca}}^{\mathrm{grt}}) - 82498{\cdot}0(X_{\mathrm{Mg}}^{\mathrm{grt}})^2(X_{\mathrm{Mn}}^{\mathrm{grt}}) \\ & - 39864{\cdot}0(X_{\mathrm{Ca}}^{\mathrm{grt}})^2(X_{\mathrm{Fe}}^{\mathrm{grt}}) - 51518{\cdot}0(X_{\mathrm{Ca}}^{\mathrm{grt}})^2(X_{\mathrm{Mg}}^{\mathrm{grt}}) \\ & - 2850{\cdot}0(X_{\mathrm{Ca}}^{\mathrm{grt}})^2(X_{\mathrm{Mn}}^{\mathrm{grt}}) - 3234{\cdot}0(X_{\mathrm{Mn}}^{\mathrm{grt}})^2(X_{\mathrm{Fe}}^{\mathrm{grt}}) \\ & - 82498{\cdot}0(X_{\mathrm{Mn}}^{\mathrm{grt}})^2(X_{\mathrm{Mg}}^{\mathrm{grt}}) - 2850{\cdot}0(X_{\mathrm{Mn}}^{\mathrm{grt}})^2(X_{\mathrm{Ca}}^{\mathrm{grt}}) \\ & - 62653{\cdot}0(X_{\mathrm{Fe}}^{\mathrm{grt}})(X_{\mathrm{Mg}}^{\mathrm{grt}})(X_{\mathrm{Ca}}^{\mathrm{grt}}) \\ & - 91682{\cdot}0(X_{\mathrm{Fe}}^{\mathrm{grt}})(X_{\mathrm{Mg}}^{\mathrm{grt}})(X_{\mathrm{Mn}}^{\mathrm{grt}}) \\ & - 24712{\cdot}0(X_{\mathrm{Fe}}^{\mathrm{grt}})(X_{\mathrm{Ca}}^{\mathrm{grt}})(X_{\mathrm{Mn}}^{\mathrm{grt}}) \\ & - 177221{\cdot}0(X_{\mathrm{Mg}}^{\mathrm{grt}})(X_{\mathrm{Ca}}^{\mathrm{grt}})(X_{\mathrm{Mn}}^{\mathrm{grt}}) \end{aligned} \quad (A3)$$

$$\begin{aligned}\mathrm{Fea} = {} & 5{\cdot}993(X_{\mathrm{Mg}}^{\mathrm{grt}})^2 - 9{\cdot}67(X_{\mathrm{Ca}}^{\mathrm{grt}})^2 - 11{\cdot}006(X_{\mathrm{Fe}}^{\mathrm{grt}})(X_{\mathrm{Mg}}^{\mathrm{grt}}) \\ & + 0{\cdot}674(X_{\mathrm{Fe}}^{\mathrm{grt}})(X_{\mathrm{Ca}}^{\mathrm{grt}}) - 9{\cdot}5725(X_{\mathrm{Mg}}^{\mathrm{grt}})(X_{\mathrm{Ca}}^{\mathrm{grt}}) \\ & - 22{\cdot}765(X_{\mathrm{Mg}}^{\mathrm{grt}})(X_{\mathrm{Mn}}^{\mathrm{grt}}) - 4{\cdot}6665(X_{\mathrm{Ca}}^{\mathrm{grt}})(X_{\mathrm{Mn}}^{\mathrm{grt}}) \\ & + 11{\cdot}006(X_{\mathrm{Fe}}^{\mathrm{grt}})^2(X_{\mathrm{Mg}}^{\mathrm{grt}}) - 0{\cdot}674(X_{\mathrm{Fe}}^{\mathrm{grt}})^2(X_{\mathrm{Ca}}^{\mathrm{grt}}) \\ & - 11{\cdot}986(X_{\mathrm{Mg}}^{\mathrm{grt}})^2(X_{\mathrm{Fe}}^{\mathrm{grt}}) + 37{\cdot}966(X_{\mathrm{Mg}}^{\mathrm{grt}})^2(X_{\mathrm{Ca}}^{\mathrm{grt}}) \\ & + 46{\cdot}02(X_{\mathrm{Mg}}^{\mathrm{grt}})^2(X_{\mathrm{Mn}}^{\mathrm{grt}}) + 19{\cdot}34(X_{\mathrm{Ca}}^{\mathrm{grt}})^2(X_{\mathrm{Fe}}^{\mathrm{grt}}) \\ & + 25{\cdot}746(X_{\mathrm{Ca}}^{\mathrm{grt}})^2(X_{\mathrm{Mg}}^{\mathrm{grt}}) + 46{\cdot}02(X_{\mathrm{Mn}}^{\mathrm{grt}})^2(X_{\mathrm{Mg}}^{\mathrm{grt}}) \\ & + 19{\cdot}145(X_{\mathrm{Fe}}^{\mathrm{grt}})(X_{\mathrm{Mg}}^{\mathrm{grt}})(X_{\mathrm{Ca}}^{\mathrm{grt}}) \\ & + 45{\cdot}53(X_{\mathrm{Fe}}^{\mathrm{grt}})(X_{\mathrm{Mg}}^{\mathrm{grt}})(X_{\mathrm{Mn}}^{\mathrm{grt}}) \\ & + 9{\cdot}333(X_{\mathrm{Fe}}^{\mathrm{grt}})(X_{\mathrm{Ca}}^{\mathrm{grt}})(X_{\mathrm{Mn}}^{\mathrm{grt}}) \\ & + 77{\cdot}876(X_{\mathrm{Mg}}^{\mathrm{grt}})(X_{\mathrm{Ca}}^{\mathrm{grt}})(X_{\mathrm{Mn}}^{\mathrm{grt}}) \end{aligned} \quad (A4)$$

$$\begin{aligned}\mathrm{Feb} = {} & -0{\cdot}034(X_{\mathrm{Mg}}^{\mathrm{grt}})^2 + 0{\cdot}135(X_{\mathrm{Ca}}^{\mathrm{grt}})^2 + 0{\cdot}024(X_{\mathrm{Mn}}^{\mathrm{grt}})^2 \\ & + 0{\cdot}1(X_{\mathrm{Fe}}^{\mathrm{grt}})(X_{\mathrm{Mg}}^{\mathrm{grt}}) + 0{\cdot}08(X_{\mathrm{Fe}}^{\mathrm{grt}})(X_{\mathrm{Ca}}^{\mathrm{grt}}) \\ & + 0{\cdot}048(X_{\mathrm{Fe}}^{\mathrm{grt}})(X_{\mathrm{Mn}}^{\mathrm{grt}}) - 0{\cdot}0515(X_{\mathrm{Mg}}^{\mathrm{grt}})(X_{\mathrm{Ca}}^{\mathrm{grt}}) \\ & + 0{\cdot}07(X_{\mathrm{Mg}}^{\mathrm{grt}})(X_{\mathrm{Mn}}^{\mathrm{grt}}) + 0{\cdot}1765(X_{\mathrm{Ca}}^{\mathrm{grt}})(X_{\mathrm{Mn}}^{\mathrm{grt}}) \\ & - 0{\cdot}1(X_{\mathrm{Fe}}^{\mathrm{grt}})^2(X_{\mathrm{Mg}}^{\mathrm{grt}}) - 0{\cdot}08(X_{\mathrm{Fe}}^{\mathrm{grt}})^2(X_{\mathrm{Ca}}^{\mathrm{grt}}) \\ & - 0{\cdot}048(X_{\mathrm{Fe}}^{\mathrm{grt}})^2(X_{\mathrm{Mn}}^{\mathrm{grt}}) + 0{\cdot}068(X_{\mathrm{Mg}}^{\mathrm{grt}})^2(X_{\mathrm{Fe}}^{\mathrm{grt}}) \\ & - 0{\cdot}136(X_{\mathrm{Mg}}^{\mathrm{grt}})^2(X_{\mathrm{Ca}}^{\mathrm{grt}}) - 0{\cdot}076(X_{\mathrm{Mg}}^{\mathrm{grt}})^2(X_{\mathrm{Mn}}^{\mathrm{grt}}) \end{aligned}$$

$$
\begin{aligned}
&-0{\cdot}27(X_{Ca}^{grt})^2(X_{Fe}^{grt})-0{\cdot}28(X_{Ca}^{grt})^2(X_{Mg}^{grt})\\
&-0{\cdot}13(X_{Ca}^{grt})^2(X_{Mn}^{grt})-0{\cdot}048(X_{Mn}^{grt})^2(X_{Fe}^{grt})\\
&-0{\cdot}076(X_{Mn}^{grt})^2(X_{Mg}^{grt})-0{\cdot}13(X_{Mn}^{grt})^2(X_{Ca}^{grt})\\
&+0{\cdot}103(X_{Fe}^{grt})(X_{Mg}^{grt})(X_{Ca}^{grt})-0{\cdot}14(X_{Fe}^{grt})(X_{Mg}^{grt})(X_{Mn}^{grt})\\
&-0{\cdot}353(X_{Fe}^{grt})(X_{Ca}^{grt})(X_{Mn}^{grt})-0{\cdot}414(X_{Mg}^{grt})(X_{Ca}^{grt})(X_{Mn}^{grt})
\end{aligned}
\tag{A5}
$$

$$
\begin{aligned}
\mathrm{Fec}=&-5672{\cdot}0(X_{Mg}^{grt})^2+19932{\cdot}0(X_{Ca}^{grt})^2+1617{\cdot}0(X_{Mn}^{grt})^2\\
&+23244{\cdot}0(X_{Fe}^{grt})(X_{Mg}^{grt})-2608{\cdot}0(X_{Fe}^{grt})(X_{Ca}^{grt})\\
&+3234{\cdot}0(X_{Fe}^{grt})(X_{Mn}^{grt})+31326{\cdot}5(X_{Mg}^{grt})(X_{Ca}^{grt})\\
&+45841{\cdot}0(X_{Mg}^{grt})(X_{Mn}^{grt})+12356{\cdot}0(X_{Ca}^{grt})(X_{Mn}^{grt})\\
&-23244{\cdot}0(X_{Fe}^{grt})^2(X_{Mg}^{grt})+2608{\cdot}0(X_{Fe}^{grt})^2(X_{Ca}^{grt})\\
&-3234{\cdot}0(X_{Fe}^{grt})^2(X_{Mn}^{grt})+11344{\cdot}0(X_{Mg}^{grt})^2(X_{Fe}^{grt})\\
&-132228{\cdot}0(X_{Mg}^{grt})^2(X_{Ca}^{grt})-82498{\cdot}0(X_{Mg}^{grt})^2(X_{Mn}^{grt})\\
&-39864{\cdot}0(X_{Ca}^{grt})^2(X_{Fe}^{grt})-51518{\cdot}0(X_{Ca}^{grt})^2(X_{Mg}^{grt})\\
&-2850{\cdot}0(X_{Ca}^{grt})^2(X_{Mn}^{grt})-3234{\cdot}0(X_{Mn}^{grt})^2(X_{Fe}^{grt})\\
&-82498{\cdot}0(X_{Mn}^{grt})^2(X_{Mg}^{grt})-2850{\cdot}0(X_{Mn}^{grt})^2(X_{Ca}^{grt})\\
&-62653{\cdot}0(X_{Fe}^{grt})(X_{Mg}^{grt})(X_{Ca}^{grt})\\
&-91682{\cdot}0(X_{Fe}^{grt})(X_{Mg}^{grt})(X_{Mn}^{grt})\\
&-24712{\cdot}0(X_{Fe}^{grt})(X_{Ca}^{grt})(X_{Mn}^{grt})\\
&-177221{\cdot}0(X_{Mg}^{grt})(X_{Ca}^{grt})(X_{Mn}^{grt})
\end{aligned}
\tag{A6}
$$

$$
\begin{aligned}
\mathrm{Mga}=&-5{\cdot}503(X_{Fe}^{grt})^2-12{\cdot}873(X_{Ca}^{grt})^2-23{\cdot}01(X_{Mn}^{grt})^2\\
&+11{\cdot}986(X_{Fe}^{grt})(X_{Mg}^{grt})-9{\cdot}5725(X_{Fe}^{grt})(X_{Ca}^{grt})\\
&-22{\cdot}765(X_{Fe}^{grt})(X_{Mn}^{grt})-37{\cdot}966(X_{Mg}^{grt})(X_{Ca}^{grt})\\
&-46{\cdot}02(X_{Mg}^{grt})(X_{Mn}^{grt})-38{\cdot}938(X_{Ca}^{grt})(X_{Mn}^{grt})\\
&+11{\cdot}006(X_{Fe}^{grt})^2(X_{Mg}^{grt})-0{\cdot}674(X_{Fe}^{grt})^2(X_{Ca}^{grt})\\
&-11{\cdot}986(X_{Mg}^{grt})^2(X_{Fe}^{grt})+37{\cdot}966(X_{Mg}^{grt})^2(X_{Ca}^{grt})\\
&+46{\cdot}02(X_{Mg}^{grt})^2(X_{Mn}^{grt})+19{\cdot}34(X_{Ca}^{grt})^2(X_{Fe}^{grt})\\
&+25{\cdot}746(X_{Ca}^{grt})^2(X_{Mg}^{grt})+46{\cdot}02(X_{Mn}^{grt})^2(X_{Mg}^{grt})\\
&+19{\cdot}145(X_{Fe}^{grt})(X_{Mg}^{grt})(X_{Ca}^{grt})\\
&+45{\cdot}53(X_{Fe}^{grt})(X_{Mg}^{grt})(X_{Mn}^{grt})\\
&+9{\cdot}333(X_{Fe}^{grt})(X_{Ca}^{grt})(X_{Mn}^{grt})\\
&+77{\cdot}876(X_{Mg}^{grt})(X_{Ca}^{grt})(X_{Mn}^{grt})
\end{aligned}
\tag{A7}
$$

$$
\begin{aligned}
\mathrm{Mgb}=&0{\cdot}05(X_{Fe}^{grt})^2+0{\cdot}14(X_{Ca}^{grt})^2+0{\cdot}038(X_{Mn}^{grt})^2\\
&-0{\cdot}068(X_{Fe}^{grt})(X_{Mg}^{grt})-0{\cdot}0515(X_{Fe}^{grt})(X_{Ca}^{grt})\\
&+0{\cdot}07(X_{Fe}^{grt})(X_{Mn}^{grt})+0{\cdot}136(X_{Mg}^{grt})(X_{Ca}^{grt})\\
&+0{\cdot}076(X_{Mg}^{grt})(X_{Mn}^{grt})+0{\cdot}207(X_{Ca}^{grt})(X_{Mn}^{grt})\\
&-0{\cdot}1(X_{Fe}^{grt})^2(X_{Mg}^{grt})-0{\cdot}08(X_{Fe}^{grt})^2(X_{Ca}^{grt})\\
&-0{\cdot}048(X_{Fe}^{grt})^2(X_{Mn}^{grt})+0{\cdot}068(X_{Mg}^{grt})^2(X_{Fe}^{grt})\\
&-0{\cdot}136(X_{Mg}^{grt})^2(X_{Ca}^{grt})-0{\cdot}076(X_{Mg}^{grt})^2(X_{Mn}^{grt})\\
&-0{\cdot}27(X_{Ca}^{grt})^2(X_{Fe}^{grt})-0{\cdot}28(X_{Ca}^{grt})^2(X_{Mg}^{grt})\\
&-0{\cdot}13(X_{Ca}^{grt})^2(X_{Mn}^{grt})-0{\cdot}048(X_{Mn}^{grt})^2(X_{Fe}^{grt})\\
&-0{\cdot}076(X_{Mn}^{grt})^2(X_{Mg}^{grt})-0{\cdot}13(X_{Mn}^{grt})^2(X_{Ca}^{grt})\\
&+0{\cdot}103(X_{Fe}^{grt})(X_{Mg}^{grt})(X_{Ca}^{grt})-0{\cdot}14(X_{Fe}^{grt})(X_{Mg}^{grt})(X_{Mn}^{grt})\\
&-0{\cdot}353(X_{Fe}^{grt})(X_{Ca}^{grt})(X_{Mn}^{grt})-0{\cdot}414(X_{Mg}^{grt})(X_{Ca}^{grt})(X_{Mn}^{grt})
\end{aligned}
\tag{A8}
$$

$$
\begin{aligned}
\mathrm{Mgc}=&11622{\cdot}0(X_{Fe}^{grt})^2+25759{\cdot}0(X_{Ca}^{grt})^2\\
&+41249{\cdot}0(X_{Mn}^{grt})^2-11344{\cdot}0(X_{Fe}^{grt})(X_{Mg}^{grt})\\
&+31326{\cdot}5(X_{Fe}^{grt})(X_{Ca}^{grt})+45841{\cdot}0(X_{Fe}^{grt})(X_{Mn}^{grt})\\
&+132228{\cdot}0(X_{Mg}^{grt})(X_{Ca}^{grt})+82498{\cdot}0(X_{Mg}^{grt})(X_{Mn}^{grt})\\
&+88610{\cdot}5(X_{Ca}^{grt})(X_{Mn}^{grt})-23244{\cdot}0(X_{Fe}^{grt})^2(X_{Mg}^{grt})\\
&+2608{\cdot}0(X_{Fe}^{grt})^2(X_{Ca}^{grt})-3234{\cdot}0(X_{Fe}^{grt})^2(X_{Mn}^{grt})\\
&+11344{\cdot}0(X_{Mg}^{grt})^2(X_{Fe}^{grt})-132228{\cdot}0(X_{Mg}^{grt})^2(X_{Ca}^{grt})\\
&-82498{\cdot}0(X_{Mg}^{grt})^2(X_{Mn}^{grt})-39864{\cdot}0(X_{Ca}^{grt})^2(X_{Fe}^{grt})\\
&-51518{\cdot}0(X_{Ca}^{grt})^2(X_{Mg}^{grt})-2850{\cdot}0(X_{Ca}^{grt})^2(X_{Mn}^{grt})\\
&-3234{\cdot}0(X_{Mn}^{grt})^2(X_{Fe}^{grt})-82498{\cdot}0(X_{Mn}^{grt})^2(X_{Mg}^{grt})\\
&-2850{\cdot}0(X_{Mn}^{grt})^2(X_{Ca}^{grt})-62653{\cdot}0(X_{Fe}^{grt})(X_{Mg}^{grt})(X_{Ca}^{grt})\\
&-91682{\cdot}0(X_{Fe}^{grt})(X_{Mg}^{grt})(X_{Mn}^{grt})\\
&-24712{\cdot}0(X_{Fe}^{grt})(X_{Ca}^{grt})(X_{Mn}^{grt})\\
&-177221{\cdot}0(X_{Mg}^{grt})(X_{Ca}^{grt})(X_{Mn}^{grt})
\end{aligned}
\tag{A9}
$$

$$
\begin{aligned}
\mathrm{Fa}=&20{\cdot}6(X_{Ab}^{pl})^2(X_{Or}^{pl})+20{\cdot}6(X_{Or}^{pl})^2(X_{Ab}^{pl})\\
&-10{\cdot}3(X_{Ab}^{pl})(X_{Or}^{pl})+20{\cdot}6(X_{Ab}^{pl})(X_{An}^{pl})(X_{Or}^{pl})
\end{aligned}
\tag{A10}
$$

$$
\begin{aligned}
\mathrm{Fb}=&-0{\cdot}788(X_{Ab}^{pl})^2(X_{Or}^{pl})-0{\cdot}788(X_{Or}^{pl})^2(X_{Ab}^{pl})\\
&+0{\cdot}24(X_{Or}^{pl})^2(X_{An}^{pl})-0{\cdot}12(X_{Or}^{pl})^2\\
&-0{\cdot}76(X_{Ab}^{pl})(X_{Or}^{pl})+1{\cdot}52(X_{Ab}^{pl})(X_{An}^{pl})(X_{Or}^{pl})
\end{aligned}
\tag{A11}
$$

$$
\begin{aligned}
\mathrm{Fc}=&-16942{\cdot}0(X_{Ab}^{pl})^2(X_{An}^{pl})-54640{\cdot}0(X_{Ab}^{pl})^2(X_{Or}^{pl})\\
&-56452{\cdot}0(X_{An}^{pl})^2(X_{Ab}^{pl})-94792{\cdot}0(X_{An}^{pl})^2(X_{Or}^{pl})\\
&-37620{\cdot}0(X_{Or}^{pl})^2(X_{Ab}^{pl})-104936{\cdot}0(X_{Or}^{pl})^2(X_{An}^{pl})\\
&+8471{\cdot}0(X_{Ab}^{pl})^2+52468{\cdot}0(X_{Or}^{pl})^2\\
&+56452{\cdot}0(X_{Ab}^{pl})(X_{An}^{pl})+100045{\cdot}5(X_{Ab}^{pl})(X_{Or}^{pl})\\
&+94792{\cdot}0(X_{An}^{pl})(X_{Or}^{pl})-200091{\cdot}0(X_{Ab}^{pl})(X_{An}^{pl})(X_{Or}^{pl}).
\end{aligned}
\tag{A12}
$$